



Jefferson Lab PAC15 Proposal Cover Sheet

This document must
be received by close
of business Thursday,

Dec 17, 1998 at:

Jefferson Lab
User Liaison,
Mail Stop 12B
12000 Jefferson Ave.
Newport News, VA
23606



Experimental Hall: B

Days Requested for Approval: 13

☐ Proposal Title:

Photon Asymmetry in $^3\text{He}(\vec{\gamma}, \pi^+) ^3\text{H}$

Proposal Physics Goals

Indicate any experiments that have physics goals similar to those in your proposal.

Approved, Conditionally Approved, and/or Deferred Experiment(s) or proposals:

E-89-017

E-93-044

Contact Person

Name: Blaine Norum

Institution: University of Virginia Physics Department

Address: 382 McCormick Road

Address:

City, State, ZIP/Country: Charlottesville, VA 22903 USA

Phone: 804-924-6789

Fax: 804-924-4576

E-Mail: ben@virginia.edu

Jefferson Lab Use Only

Receipt Date: 12/17/98

By: to. Amick

PR 99-009

HAZARD IDENTIFICATION CHECKLIST

JLab Proposal No.: _____

(Per CBMF User Liaison Office use only.)

Date: _____

Check all items for which there is an anticipated need.

Cryogenics <input type="checkbox"/> beamline magnets <input type="checkbox"/> analysis magnets <input checked="" type="checkbox"/> target type: _____ flow rate: _____ capacity: _____	Electrical Equipment <input type="checkbox"/> cryo/electrical devices <input type="checkbox"/> capacitor banks <input type="checkbox"/> high voltage <input type="checkbox"/> exposed equipment	Radioactive/Hazardous Materials List any radioactive or hazardous/toxic materials planned for use: _____ _____ _____
Pressure Vessels <input type="checkbox"/> inside diameter <input type="checkbox"/> operating pressure <input type="checkbox"/> window material <input type="checkbox"/> window thickness	Flammable Gas or Liquids type: _____ flow rate: _____ capacity: _____ Drift Chambers type: _____ flow rate: _____ capacity: _____	Other Target Materials <input type="checkbox"/> Beryllium (Be) <input type="checkbox"/> Lithium (Li) <input type="checkbox"/> Mercury (Hg) <input type="checkbox"/> Lead (Pb) <input type="checkbox"/> Tungsten (W) <input type="checkbox"/> Uranium (U) <input type="checkbox"/> Other (list below) _____ _____
Vacuum Vessels <input type="checkbox"/> inside diameter <input type="checkbox"/> operating pressure <input type="checkbox"/> window material <input type="checkbox"/> window thickness	Radioactive Sources <input type="checkbox"/> permanent installation <input type="checkbox"/> temporary use type: _____ strength: _____	Large Mech. Structure/System <input type="checkbox"/> lifting devices <input type="checkbox"/> motion controllers <input type="checkbox"/> scaffolding or <input type="checkbox"/> elevated platforms
Lasers type: _____ wattage: _____ class: _____ Installation: <input type="checkbox"/> permanent <input type="checkbox"/> temporary Use: <input type="checkbox"/> calibration <input type="checkbox"/> alignment	Hazardous Materials <input type="checkbox"/> cyanide plating materials <input type="checkbox"/> scintillation oil (from) <input type="checkbox"/> PCBs <input type="checkbox"/> methane <input type="checkbox"/> TMAE <input type="checkbox"/> TEA <input type="checkbox"/> photographic developers <input type="checkbox"/> other (list below) _____ _____	General: Experiment Class: <input type="checkbox"/> Base Equipment <input type="checkbox"/> Temp. Mod. to Base Equip. <input checked="" type="checkbox"/> Permanent Mod. to Base Equipment <input checked="" type="checkbox"/> Major New Apparatus Other: _____ _____

LAB RESOURCES LIST

JLab Proposal No.: _____ Date _____

(For JLab ULO use only.)

List below significant resources — both equipment and human — that you are requesting from Jefferson Lab in support of mounting and executing the proposed experiment. Do not include items that will be routinely supplied to all running experiments such as the base equipment for the hall and technical support for routine operation, installation, and maintenance.

Major Installations *(either your equip. or new equip. requested from JLab)*

Coherent Bremsstrahlung Photon Source

New Support Structures: _____

Data Acquisition/Reduction

Computing Resources: _____

New Software: _____

Major Equipment

Magnets: _____

Power Supplies: _____

Targets: L^3He - 1.5 cm diameter cell

Detectors: _____

Electronics: _____

Computer Hardware: _____

Other: _____

Other: _____

BEAM REQUIREMENTS LIST

Lab Proposal No.: _____ Date: _____

Hall: _____ Anticipated Run Date: _____ PAC Approved Days: _____

Spokesperson: B. Norum, J. Calarco, K. Wang Hall Liaison: _____

Phone: 804-924-6789

E-mail: ben@virginia.edu

List all combinations of anticipated targets and beam conditions required to execute the experiment. (This list will form the primary basis for the Radiation Safety Assessment Document (RSAD) calculations that must be performed for each experiment.)

[illegible]

The beam energies, E_{beam} , available are: $E_{\text{beam}} = N \times E_{\text{Linac}}$ where $N = 1, 2, 3, 4$, or 5 . $E_{\text{Linac}} = 800$ MeV, i.e., available E_{beam} are 800, 1600, 2400, 3200, and 4000 MeV. Other energies should be arranged with the Hall Leader before listing.

Photon Asymmetry in ${}^3\text{He}(\vec{\gamma}, \pi^+) {}^3\text{H}$

A. Cichocki, D. Higinbotham,

R. A. Lindgren, B. E. Norum, C. Smith, and K. Wang
University of Virginia, Charlottesville, Virginia

J. R. Calarco

University of New Hampshire, Durham, New Hampshire

R. S. Hicks, D. Lawrence, R. A. Miskimen

G. A. Peterson and J. Shaw

University of Massachusetts, Amherst, MA

H. Crannell, A. Longhi, J. O'Brien, D. Sober

Catholic University of America, Washington, D.C.

J. Chen, J. Mitchell, and E. Smith

Jefferson Lab, Newport News, Virginia

C. Bennhold, W. Briscoe, P. Cole, and K. Dhuge

George Washington University, Washington, D.C.

H. Weller

Duke University, Durham, NC

J. Ficenec and D.A. Jenkins

Virginia Polytechnic Institute and State University, Blacksburg, Virginia

R. Ent, and C. Keppel

Hampton University, Hampton, Virginia

T. P. Welch

Oregon State University, Corvallis, Oregon

D. Beatty, T. Fortune, W. Lorenzon and J. Yu

University of Pennsylvania, Philadelphia, PA

J. Napolitano and P. Stoler

Rensselaer Polytechnic Institute, Troy, NY

AND THE REAL PHOTON GROUP OF CLAS

December 17, 1998

Abstract

We propose to study the reaction ${}^3\text{He}(\gamma, \pi^+) {}^3\text{H}$ at momentum transfers, Q^2 , ranging up to 20 fm^{-2} using polarized photons with energies between 300 MeV and 650 MeV. Both the differential cross section, $d\sigma/d\Omega_\pi$, and the photon asymmetry, Σ , will be measured. The broad kinematic range spanned by the data will enable us to investigate a possible breakdown of DWIA arising from two-body mechanisms and possible changes in elementary amplitudes, the influence of two-step processes in the ${}^3\text{He}$ nucleus, and the magnitude of D-state components in the nuclear three-body wave function. Of these, the principal focus will be on the possible breakdown of the impulse approximation arising from modifications of the $E_{1+}(\Delta)$ amplitude in a dense nuclear system. The D-wave admixture in the trinucleon wave function gives rise to a potentially large SD interference contribution to Σ . This contribution is approximately proportional to the $E_{1+}(\Delta)$ amplitude so the photon asymmetry Σ provides a sensitive measure of the $E_{1+}(\Delta)$ amplitude. However, the extraction of such effects will require a simultaneous, accurate determination of the D-wave admixture. The contributions of each of these factors to the cross section and to the photon asymmetry have characteristic dependencies upon photon energy, photon polarization, and pion emission angle. Isolation of a particular contribution will require simultaneous analysis of data over a broad kinematic range. As a result, the experiment will require the unique combination of properties provided by the CLAS detector and the Coherent 0 Source or the proposed Compton High Intensity Photon Source, should it become available.

1 Introduction

A principal goal of nuclear physics is to understand how nucleons and nucleonic processes are affected by the presence of other nucleons in a nuclear medium. To study this question amplitudes for a process involving a nucleus are compared to those for the corresponding process on a free nucleon. The results of such comparisons can be sensitive to several distinct effects. In the case of charged pion photoproduction these include the presence of meson-exchange or other two-body currents in the nucleus, pion-nucleus rescattering, details of the nuclear wave function, final state interactions between the outgoing pion and residual nucleus, and possible differences in the elementary amplitudes. The magnitude of the effect of each of these depends upon the kinematics of a particular measurement and upon the observable being measured: total cross section (σ), differential cross section ($d\sigma/d\Omega$), photon asymmetry (Σ), etc. If the contributions for all but one of these effects are known for a particular measurement, then that measurement can yield new information about the remaining effect.

One question that can be addressed in this manner relates to the properties of the nucleonic resonances. Total photoabsorption data from Frascati[1] indicate that excitation of the Δ resonance appears to be unaffected by whether the nucleon involved is in a nucleus or not. By contrast, the higher resonances such as the D_{13} which appear prominently in photoabsorption on the proton are washed out completely in photoabsorption on a nucleus. This can be understood qualitatively by noting that the Δ excitation is dominated by the M_{1+} spin-flip amplitude whereas the higher resonances correspond to spatial excitations. The amplitude for flipping the spin of one quark should, to first approximation, be independent of changes in the spatial wave function whereas the amplitude for a quadrupole excitation, for example, should be quite sensitive. It follows that if one wants to look for effects of the nuclear medium on the Δ excitation process one should look at the quadrupole component, the E_{1+} amplitude. The photon asymmetry, Σ , in the reaction ${}^3\text{He}(\gamma, \pi^+) {}^3\text{H}$ is particularly sensitive to this amplitude; examining this amplitude is, therefore, the principal focus of the proposed experiment. Other effects, such as the presence of meson-exchange or other two-body currents, pion-nucleus rescattering, and final state interactions between the outgoing

pion and residual nucleus will also be studied both for the need to control them in order to isolate the effect of the E_{1+} amplitude as well as for their own intrinsic interest.

The ${}^3\text{He}$ nucleus is an ideal target for such studies. It is the simplest nucleus wherein the nucleons are bound tightly together and for which the nuclear structure is relatively well understood. Precise, correlated three-body wave functions can be obtained using, for example, the Faddeev approach calibrated to electron scattering and other data. There remains, however, a significant uncertainty in the amplitude of the D-state in the 3-body ground state. Inasmuch as this amplitude largely determines the magnitude of the effect of the $E_{1+}(\Delta)$ on the photon asymmetry it is crucial that it be determined accurately. Fortunately, there are kinematic regions covered in the proposed experiment where both the differential cross section and the photon asymmetry are very sensitive to the D-state and extremely insensitive to the Δ . Thus, we will measure the D-state amplitude in this experiment; its determination will constitute a second major focus of the work.

The situation with a ${}^3\text{He}$ target contrasts with the case of heavier nuclei where the single particle wave functions are computed using the shell model, or other similarly phenomenological model in which effective nuclear structure parameters are constrained by β -decay rates, electromagnetic form factors, and other experimental observables. In these cases, nontrivial ambiguities are inevitable, especially in magnetic transitions. In order to isolate reliably the effects of interest from the effects of nuclear structure it is necessary to know both the initial and final nuclear states. The most effective way to do this is to require that the recoiling nucleons stay integrated as ${}^3\text{He}$. Thus, with respect to isospin the reaction is essentially an “elastic” or “iso-elastic” process as opposed to an “inelastic” process wherein the ${}^3\text{He}$ is broken apart.

The earliest experimental study of the ${}^3\text{He}(\gamma, \pi^+) {}^3\text{H}$ reaction was performed in the 1960's [2] at the University of Illinois with 180 MeV to 260 MeV photons produced by bremsstrahlung radiation. The measured cross sections were found to be generally well described by impulse approximation. However, when examined in detail, the cross sections were observed to lie from 25% to 60% below the simple theory. The discrepancy was attributed to inaccurate wave functions and a suppression of pion production in nuclear

matter.

Another experiment was performed using a bremsstrahlung beam at Saclay in the 1970's [3]. The differential cross section could be described at small momentum transfers by the impulse approximation with Faddeev wave functions. However, as the momentum transfer was increased to above 6 fm^{-2} , a discrepancy between the data and a calculation using the distorted-wave impulse approximation (DWIA) appeared. A complete calculation with a novel two-body contribution was required to give a full description [4] of the data. Significantly, this two-body formalism predicts that at higher photon energies, such as 400 MeV and above, the two-body contribution constitutes almost the entire cross section.

Subsequently, the measurement was repeated at Saclay but this time using a positron-annihilation photon source which provided quasi-monochromatic photons [5]. In addition to the iso-elastic process, two-body and three-body break up channels were also studied. The energy of the photon beam was from 210 MeV to 450 MeV. The angles at which pions were detected ranged from 20° to 72° , corresponding to momentum transfers from 0.28 fm^{-2} to 3.0 fm^{-2} . For the data at higher momentum transfer calculations including the two-step charge-exchange process, ${}^3\text{He}(\gamma, \pi^0){}^3\text{He}(\pi^0, \pi^+){}^3\text{H}$, gave a better description.

The experiment was also performed at Bonn using the bremsstrahlung beam of the 500 MeV synchrotron [6]. The recoiling nuclei were detected in coincidence with the produced pion permitting a clean isolation of the iso-elastic process. The cross sections in these measurements were found to be lower than the theoretical calculations, indicating that the understanding of the reaction is incomplete.

Theoretical work on this reaction was initially performed within the framework of the plane-wave impulse approximation(PWIA) [7, 8]. These calculations were followed by DWIA calculations [9] which included the pion rescattering contribution. Later calculations by Laget [10] explicitly included both real and imaginary components in both the M_{1+} and E_{1+} multipoles. Most recently, Kamalov, Tiator and Bennhold [11, 12] (KTB) have carried out a general study of polarization observables for this reaction. These cal-

culations, which include the Δ and higher resonances (S_{11} , P_{11} , P_{33} , D_{13} , F_{15} , and D_{33}), were performed within a newly developed coupled-channels framework [9] which can consistently describe elastic π^+ and coherent π^0 photoproduction as well as elastic and charge-exchange pion scattering from ^3He . The KTB calculation successfully reproduced the cross section of the $^3\text{He}(\gamma, \pi^+) ^3\text{H}$ data [6, 11, 13, 14] over a wide range of photon energies and momentum transfers. The most attractive parts of the calculation are the single polarization observables Σ (photon asymmetry), T (target polarization asymmetry) and P (recoil polarization asymmetry). These polarization observables contain interference terms of the various reaction amplitudes in different combinations and may be more sensitive to small amplitudes of interesting dynamic effects. With a polarized photon beam much more information on the dynamics of the system can be extracted than is possible with unpolarized beams. The calculations show that the photon asymmetry Σ is very sensitive to details of the trinucleon wave function (such as D-state components) and the E_{1+} amplitude of the delta. Consequently, a study of the $^3\text{He}(\gamma, \pi^+) ^3\text{H}$ reaction will enable us to access important issues inaccessible using unpolarized photons.

Until recently, the full capabilities of the photon as a probe of nuclear systems have not been realizable due to technical limitations. While high fluxes of high energy, unpolarized photons have been available from a variety of bremsstrahlung sources, similar fluxes of linearly polarized photons have not. During the last few years linearly polarized photon beams obtained from both bremsstrahlung and Compton backscattering sources have become available. Unfortunately, in the case of bremsstrahlung sources the polarization is significant only for a relatively narrow range of photon energies at about $\frac{1}{3}$ to $\frac{1}{2}$ of the maximum photon energy. In addition, the degree of polarization is often modest $\approx 50\%$, although this can be increased significantly (approaching 85%) at the expense of energy range and tagging efficiency. Existing and most planned Compton backscattering sources are operated as parasitic operations at synchrotron light sources [15]. Consequently, while they have the very desirable properties of high polarization at the highest photon energies, very high tagging efficiency, and a broad range of energies at which the polarization is significant, their fluxes are very limited by constraints on how many electrons they can remove from the rings. Also, the energy resolution of these beams is poor, ranging from about 5.5 MeV at LEGS to 15 MeV at

GRAAL.

We plan to perform measurements of the differential cross sections and photon asymmetries in Hall B using either the coherent bremsstrahlung source currently under development[16] or the proposed Compton backscattering facility [17], should it become available. We will use the liquid ^3He target designed by the Saclay group [18] and the CLAS detector. The CLAS will permit detection of π^+ 's emitted in a wide angular range. With the anticipated momentum resolution, the iso-elastic peak will be clearly separable from the two- and three-body break up channels. At higher energies and backward π^+ production angles, it will also be possible to detect the recoiling ^3He . This will completely suppress all other backgrounds under those kinematic conditions where the cross section is smallest. The excellent track reconstruction properties of the CLAS will enable us to use a long target, thereby maximizing the luminosity and counting rate. Significantly, the small transverse dimensions of the γ beam will enable us to use a target with a small transverse extent, thereby minimizing the material through which reaction products must pass and minimizing the degradation of track reconstruction capabilities that results from multiple scattering.

These technologies are ideally suited to this measurement. The combination of photon beam, detector, and target makes Hall B at JLAB the only place where this experiment is feasible.

2 Physics Motivation

The most important quantity to be measured is the polarized photon asymmetry, defined by

$$\Sigma = \left(\frac{1}{P_l} \right) \left[\frac{d\sigma/d\Omega^\perp - d\sigma/d\Omega^\parallel}{d\sigma/d\Omega^\perp + d\sigma/d\Omega^\parallel} \right],$$

where the superscript \perp (\parallel) refers to photons linearly polarized perpendicular (parallel) to the reaction plane and P_l is the polarization of the incoming photon beam. In a very simple model based on an harmonic-oscillator S-shell nuclear wave function, the photon asymmetry for ${}^3\text{He}(\vec{\gamma}, \pi^+) {}^3\text{H}$ and a nucleon process $p(\vec{\gamma}, \pi^+)n$ can be related simply by

$$\Sigma({}^3\text{He}) = \Sigma(p).$$

However, this is true only for a naive model in which only the S-wave component in the ${}^3\text{He}$ wave functions is considered. In a realistic model, the D-wave component can drastically affect this equality. The most extensive calculation of this quantity for the reaction ${}^3\text{He}(\vec{\gamma}, \pi^+) {}^3\text{H}$ has been carried out by Kamalov, Tiator, and Bennhold [11]. In calculating Σ a trinucleon wave function in momentum space is used. It is dominated by the S-state amplitude (90%) while the D-state contributes about 8%. If only the major S-wave components and the lowest pion-nucleon s- and p-waves in the amplitude $t_{\gamma N}$ are considered, the photon asymmetry can be expressed in terms of the $\gamma + N$ multipoles $E_{l\pm}$ and $M_{l\pm}$ as

$$\Sigma_S = \frac{\pi \sin^2 \theta}{d\sigma_A/d\Omega} \left[M_{00}^2(Q) |2M_{1+} + M_{1-}|^2 - \frac{1}{3} M_{10}^2(Q) |f_{em}|^2 \right] W_A, \quad (1)$$

where W_A is a kinematic factor, $f_{em} = 3E_{1+} - M_{1+} + M_{1-}$, $M_{SLJ}(Q)$ are nuclear form factors, S and L are the spin and orbital angular momentum of the nucleon pair inside the trinucleon system, θ is the pion emission angle, and J is the angular momentum transfer in the scattering process, with $J = 0$ for non-spin-flip and $J = 1$ for spin-flip processes.

When the D-wave component is included, additional contributions to the photon asymmetry arise, one important part coming from the interference

between the S- and D-state components. The KTB theory offers an explicit expression for this contribution at $\theta_{c.m.} = 90^\circ$ in terms of the elementary multipoles:

$$\Sigma_{SD}(90^\circ) = \frac{\sqrt{2}\pi}{Q^2 d\sigma_A/d\Omega} M_{101}(Q) M_{121}(Q) [2qk \Re E_{0+} f_{em}^* - q^2 |E_{0+}|^2 - (4k^2 + q^2) |f_{em}|^2 W_A] \quad (2)$$

$$(4)$$

where q and k are the momentum of the pion and photon respectively and Q is the momentum transfer. The SD interference term contains a large E_{0+} multipole, which does not exist with an S-wave function alone. Therefore, an enhancement of D-state contribution will lead to a modification of the photon asymmetry. The first term in the square brackets in equation 3 gives an interference of E_{0+} and E_{1+} multipoles due to the presence of a D-state component. This interference will increase the sensitivity of the photon asymmetry to the $E2(\Delta)$ transition. It should be noted that this effect is rather small in the differential cross section due to the large background produced by the E_{0+} and M_{1+} multipoles.

The E_{0+} appearing here is that for charged pion production. It is, of course, much larger than that for π^0 production and is the reason that we use charged pion production to study Δ properties rather than the more commonly used π^0 production.

Figures 1 and 2 show the differential cross sections at $\theta = 90^\circ$ and $\theta = 120^\circ$ for photon energies up to 650 MeV from a calculation in which the contributions from different components are compared [12]. The reaction is dominated by S-wave at low energies, $E_\gamma < 450$ MeV. As the photon energy increases, the contribution of the D-state component in ${}^3\text{He}$ becomes larger, for $E_\gamma = 560$ MeV and $\theta = 90^\circ$, D-state component increases the cross section by almost an order of magnitude. At backward angles, the effect of D-state component starts at lower energies and becomes 0 above 450 MeV. One can also see that the effect E_{1+} multipole on the cross section is generally small.

The KTB theory predicts that the sensitivity of the photon asymmetry to the $E2(\Delta)$ transition is enhanced when using the full wave function in contrast to using only the S-state components. Figures 3 and 4 show the energy

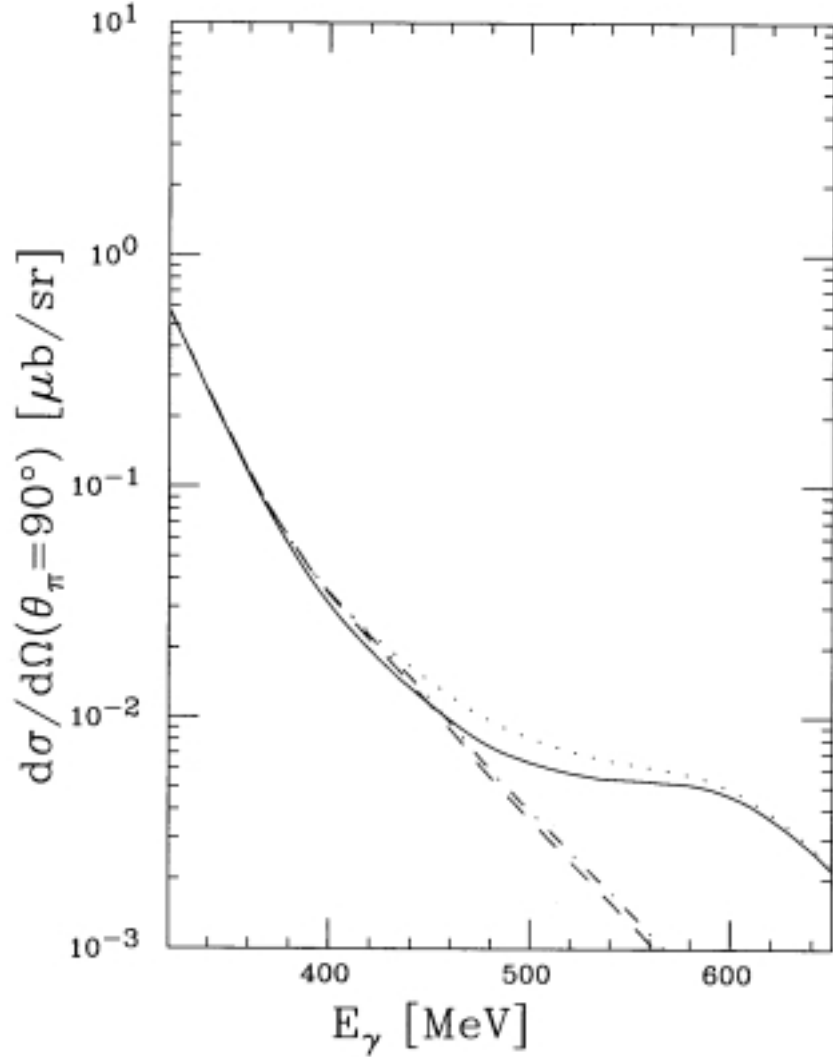


Figure 1: Calculated energy dependence of the differential cross section at $\theta = 90^\circ$. The solid (dashed) curve was calculated with (without) D-state components in the three-body wave function and the full production operator. The dash-dotted (dotted) curve was calculated with (without) D-state components in the three-body wave function but without the $E_{1+}(\Delta)$ multipole in the production operator.

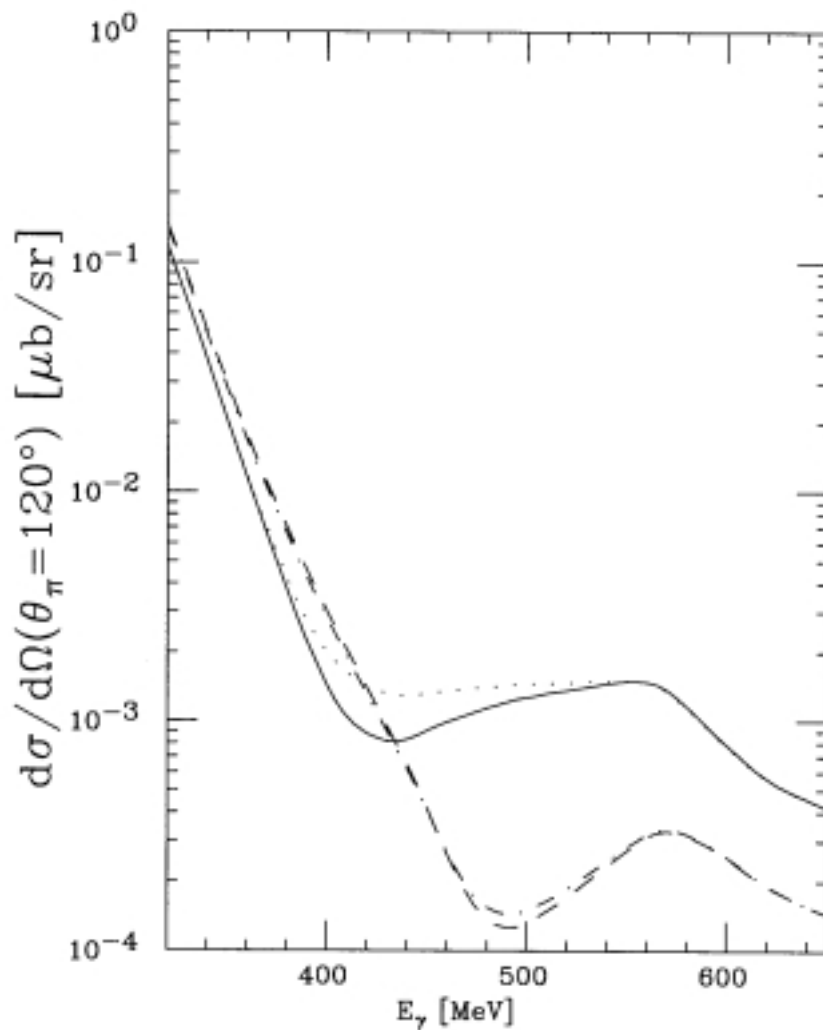


Figure 2: Calculated energy dependence of the differential cross section at $\theta = 120^\circ$. The solid (dashed) curve was calculated with (without) D-state components in the three-body wave function and the full production operator. The dash-dotted (dotted) curve was calculated with (without) D-state components in the three-body wave function but without the $E_{1+}(\Delta)$ multipole in the production operator.

dependence of the photon asymmetry from the same calculation at $\theta_\pi = 90^\circ$ and $\theta_\pi = 120^\circ$. Obviously, the D-wave components and the $E_{1+}(\Delta)$ multipoles cause a drastic change. At $\theta_\pi = 90^\circ$, involving the D-wave shifts the node of photon asymmetry from 500 MeV down to 430 MeV and the energy for maximal asymmetry 580 MeV down to 500 MeV. However, the effect of the $E_{1+}(\Delta)$ multipoles is not large enough to be observed experimentally. At $\theta_\pi = 120^\circ$, the effect $E_{1+}(\Delta)$ multipoles is large enough to be extracted in the region from 400 MeV to 500 MeV.

The KTB theory uses a coupled-channel calculation to account for the final state interaction (FSI). The largest contribution of the two-step process $(\gamma, \pi^0)(\pi^0, \pi^+)$ comes from the coherent non-spin-flip transition in the (γ, π^0) channel with subsequent spin-flip transition in the (π^0, π^+) channel. Therefore, the spin degrees of freedom in the pion-nuclear interaction significantly affect polarization observables in charged-pion photoproduction at backward angles.

In examining the disagreement between the experimental and theoretical cross sections, Kamalov *et al.*[4] developed a two-body mechanism which reproduces the cross section data [3, 5, 14]. PWIA works well for low momentum transfers, but as Q^2 increases to 6 fm^{-2} the agreement worsens and it cannot be recovered by including pion rescattering. The introduced two-body mechanism, arising mainly from the isovector magnetic components of the two-body operator, raises the cross section by up to two orders of magnitude. Figure 5 shows the theoretical predictions at 400 MeV. One can see that at 120° the cross section is enhanced by a factor of 10 when the two-body mechanism is included.

Recently, Gómez *et al.*[19] performed a new calculation of the meson exchange currents (MEC) mechanism in nuclei starting from the $\gamma N \rightarrow \pi\pi N$ amplitude. In their model, one of the pions is produced off-shell from one nucleon and is absorbed by another nucleon. Their results showed that the cross section at large momentum transfers is dominated by the two-body current and that the MEC's produce important effects in the photon asymmetry in the Δ resonance region. For 300 MeV photons, the photon asymmetry can be increased by a factor of two around 50° to 120° .

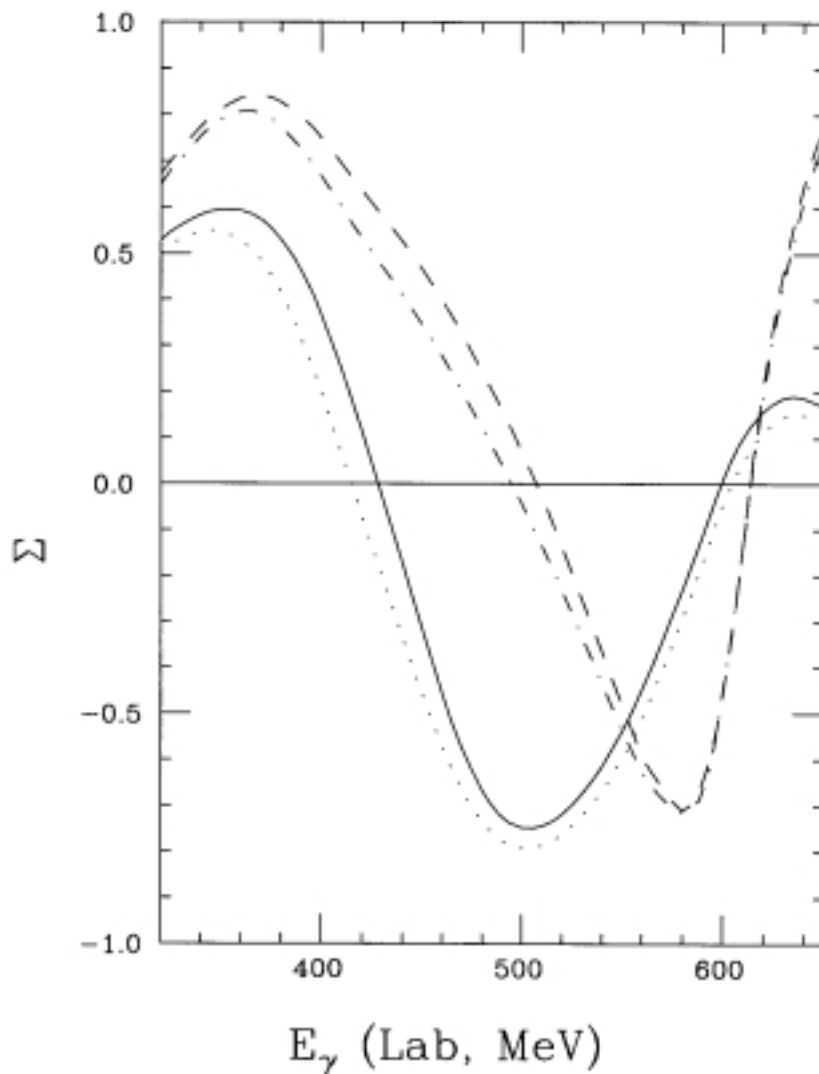


Figure 3: Calculated energy dependence of the photon asymmetry at $\theta = 90^\circ$. The solid (dashed) curve was calculated with (without) D-state components in the three-body wave function and the full production operator. The dash-dotted (dotted) curve was calculated with (without) D-state components in the three-body wave function but without the $E_{1+}(\Delta)$ multipole in the production operator.

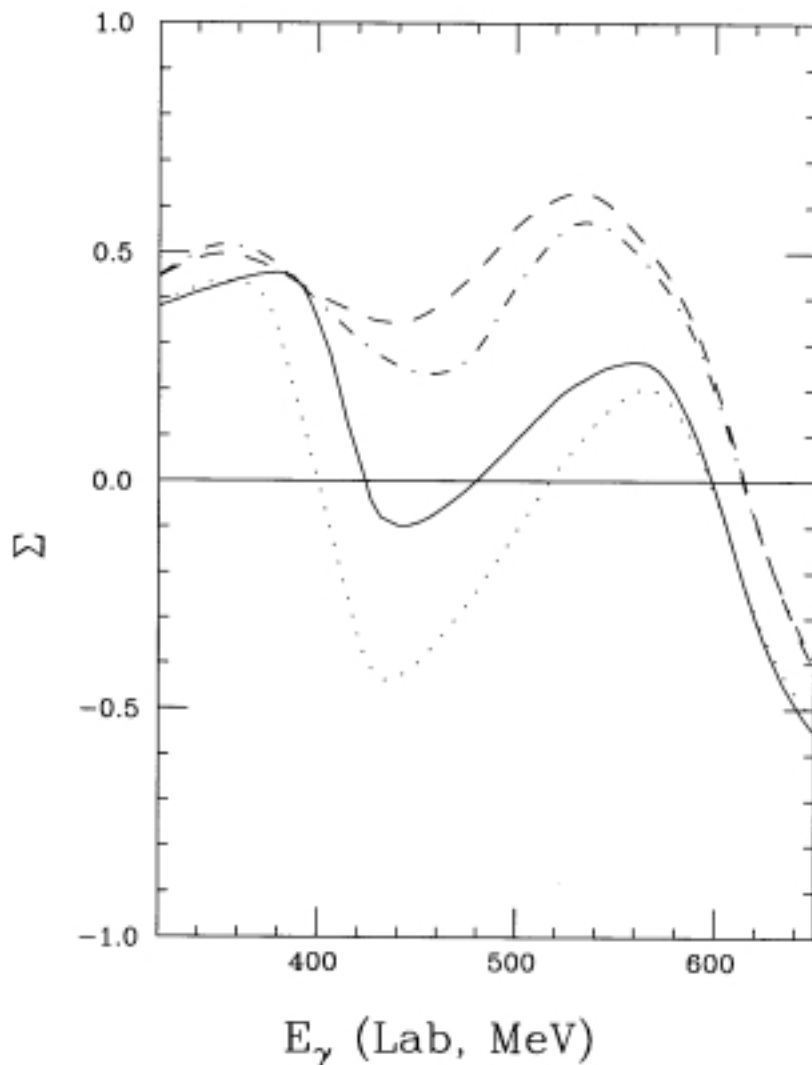


Figure 4: Calculated energy dependence of the photon asymmetry at $\theta = 120^\circ$. The solid (dashed) curve was calculated with (without) D-state components in the three-body wave function and the full production operator. The dash-dotted (dotted) curve was calculated with (without) D-state components in the three-body wave function but without the $E_{1+}(\Delta)$ multipole in the production operator.

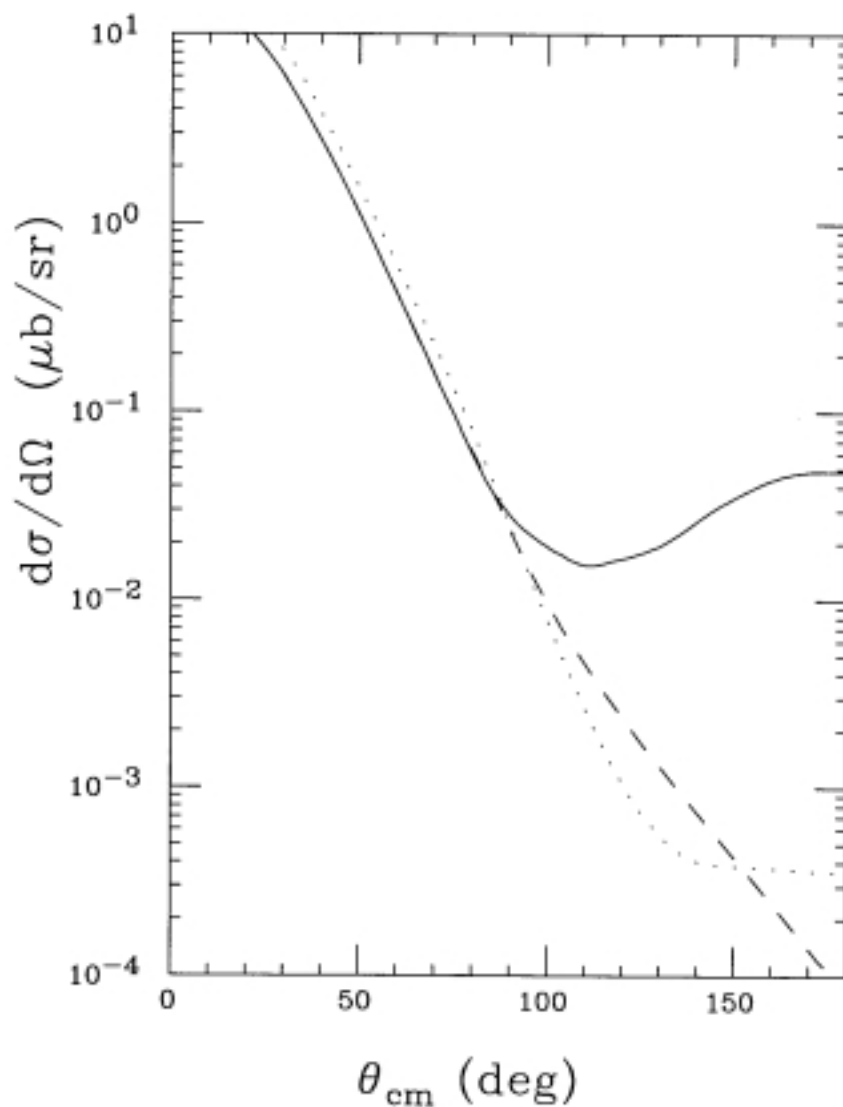


Figure 5: Pion angular distribution for an incident photon energy of 400 MeV. The dotted (dashed) curves show the PWIA (DWIA) results obtained with Faddeev wave functions. The full line shows the KTB complete calculation with the two-body mechanism.

In summary, potentially rich physics is contained in the combination of precise cross section and photon asymmetry measurements. With a polarized photon beam and a large acceptance detector it will be possible to study this physics by measuring the cross section and photon asymmetry over a wide range of energies and angles. The cross section data at all energies and angles will enable us to determine the effects of distortions, two-body currents, and multi-step processes. The photon asymmetry and the cross section data at forward to middle angles will enable us to determine the D-state contributions. The photon asymmetry data at more backward angles will provide a determination of the $E_{1+}(\Delta)$ amplitude in a nuclear system. It is expected that by the time this experiment is performed the E_{1+} amplitude on the free nucleon will be precisely known. Our results then will provide a sensitive measure of the effect of the nuclear medium on the Δ .

3 Experimental Approach

The proposed experimental study of photon asymmetry in ${}^3\text{He}(\gamma, \pi^+){}^3\text{H}$ will require a polarized photon source, a large acceptance detector with good resolution, and a cryogenic liquid ${}^3\text{He}$ target. This section will be devoted to a discussion of the photon source, the CLAS detector, the target, and a Monte Carlo simulation of the experiment.

3.1 Photon Beam, ${}^3\text{He}$ Target, and Detector

Two options for the γ source are under consideration. The first choice is the Coherent Bremsstrahlung Source (CBS) which is currently under development; the second choice is the proposed Compton High Intensity Photon Source (CHIPS). The former has the distinct advantage of having already been approved and funded. The latter promises a higher figure of merit for this experiment and a generally higher quality beam. The CBS is expected to produce polarizations in excess of 75% over a restricted range of energies; photons are still generated across the entire energy range but the rest are unpolarized. The concentration of γ 's in a narrow range necessitates adjusting the system, crystal orientation and/or electron beam energy, for each energy across the range to be covered in the experiment. As a result, these changes represent lost measurement time. However, they do introduce two advantages. First, the photon polarization can be kept high for all photon energies unlike the case of the CHIPS with which the polarization for the lowest photon energies would be significantly lower than 75%. Second, the time spent measuring at each energy setting can be varied to equalize the precision of the measurement for all energies.

The target to be used is the liquid ${}^3\text{He}$ target designed and constructed by the Saclay group [18]. The target cell is 20 cm long, is nominally 4.3 cm in diameter, and is constructed of 170 μm mylar foil. Because of the very small size of the γ beam the diameter will be reduced to between 1 cm and 2 cm.

The CLAS detector will be used in this measurement. Its features include large acceptance, charged particle tracking, momentum mapping, and parti-

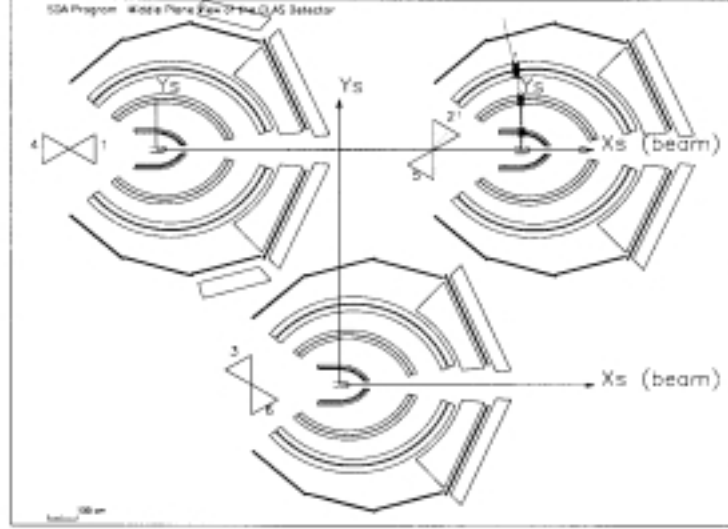


Figure 6: Typical simulated event of $\gamma^3\text{He} \rightarrow \gamma\pi^+{}^3\text{H}$ from SDA with $E_\gamma = 500 \text{ MeV}$, $\theta_\pi = 90^\circ$.

cle identification by TOF. It covers almost all of the kinematic region containing the physics that this experiment is intended to explore. The trigger for this experiment will consist of a coincidence between the tagging spectrometer and a start counter placed around the target. This start counter is composed of three pieces of plastic scintillator each 3 mm thick [20]. Figure 3.1 shows a typical event from an SDA simulation for $E_\gamma = 500 \text{ MeV}$ and $\theta_\pi = 90^\circ$.

The π^+ will be detected by the start counter and then will be tracked by the three regions of drift chambers, where its momentum and its charge will be determined. Finally, it will be detected by the TOF counter. In general, it will not be possible to detect the recoiling ${}^3\text{H}$, but when the photon energy is above 450 MeV, some higher energy ${}^3\text{H}$'s ($E_K > 60 \text{ MeV}$) can reach the TOF counter and be identified. Particles (π^- , π^0 , p, and d) emerging from

other reaction channels also will be identified and measured. These data will permit the examination of issues related to the two- and three-body breakup channels (not addressed in this proposal) as well as being useful in rejecting background events.

Figure 7 shows the angular distribution of the pion momentum in the laboratory system. The approximately vertical dotted curves are the corresponding center mass emission angles. One can see that in the energy range of interest for this experiment, the moment lie between 200 MeV/c and 700 MeV/c. With the CLAS detector, data will be acquired for center mass angles between about 10° and 130° .

3.2 Resolution

Over most of the kinematic range, identification of the iso-elastic reaction channel will rely solely upon the detection of a single π^+ . The missing mass associated with the undetected recoiling nucleons will determine whether the reaction that produced the π^+ was an iso-elastic or inelastic process. The thresholds for two-body and three-body disintegration of ^3He are 6.78 MeV and 8.48 MeV, respectively, so a missing mass resolution of about 5 MeV is required. For photon energies between 300 MeV and 650 MeV, the resultant pion momenta range from 220 MeV/c to 630 MeV/c. At these momenta the CLAS has a momentum resolution of about 1.0% (FWHM).

In modeling the experiment to obtain a better determination of the missing mass resolution, it was assumed that the energy distribution of the photons has an gaussian shape with an FWHM of 2 MeV. The azimuthal angle ϕ_* in laboratory system was randomly generated across the full range of 2π and the pion momentum was fixed by the iso-elastic kinematics. The SDA code [21] was used for the Monte Carlo simulation. The two-body breakup events were generated separately using the model described in [13]. This model assumes quasi-free photon absorption process on a proton in the target nucleus. Accordingly, the cross section has the same general features as that for π^+ photoproduction on a free nucleon but is shifted and spread by the binding energy and Fermi motion in ^3He .

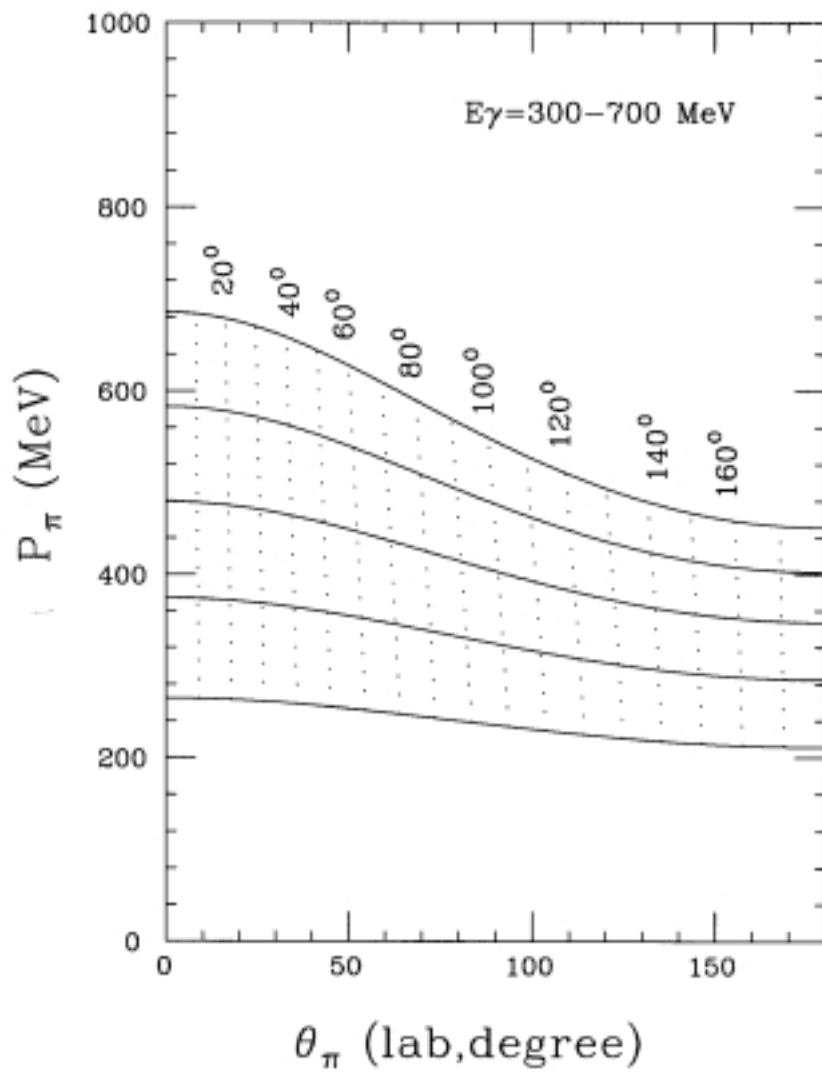


Figure 7: Pion momentum angular distribution in the laboratory frame for E_γ from 300 MeV to 700 MeV. The approximately vertical dotted curves are the corresponding center mass emission angles.

Figure 8 shows the momentum spectrum for pions produced at 40.6° by photons with an energy of 338 MeV. A clear separation between the iso-elastic peak and the broad quasi-free peak can be seen. As a comparison, the spectrum at the same energy and angle from the Saclay data of d'Hose *et al.* [13] is shown in figure 9.

Figures 10 and 11 (12 and 13) show momentum spectra for pions produced by 350 MeV (450 MeV) photons and emitted at 90° and 120° . From the spectra, one can see that at forward angles, the elastic peak is getting closer to the bump of the two-body break up. The two peaks can be well separated with the CLAS detector for polar angles of 30° . For backward scattering, the requirement on momentum resolution is less severe.

Figure 14 shows the simulated missing mass spectrum corresponding to an incident photon energy of 450 MeV and a pion emission angle of 90° . From these Monte Carlo simulations it was determined that the resolution is adequate to separate the iso-elastic peak from two-body and three-body break up processes. In the experiment, it will be necessary to group the data into bins in the polar angle θ_π of at least 1° in width. The effect of this binning on our ability to separate iso-elastic from inelastic channels depends upon the dependence of pion momentum on pion angle. This dependence is shown in figure 15 where, in most cases, the derivative of the momentum to angle is less than $1 \text{ MeV}/^\circ$. Polar angle bin widths of a few degrees will be possible at larger angles.

3.3 Acceptance

In order to evaluate the solid angle acceptance, iso-elastic events corresponding to each photon energy were generated and distributed uniformly over a polar angle range from 10° to 120° . With photon energies between 300 MeV and 650 MeV this angular range corresponds to a Q^2 range from 0.08 fm^{-2} to 20 fm^{-2} . The acceptance obtained from SDA is listed in table 4. Figure 16 shows the acceptance as a function of pion momentum. Figure 17 shows the dependence of Q^2 on c.m. pion emission angle for different photon energies.

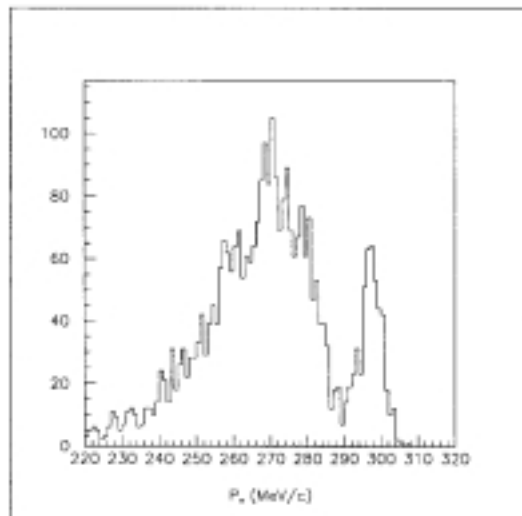


Figure 8: Pion momentum spectra for $E_\gamma = 338 \text{ MeV}$ at $\theta_\pi = 40.6^\circ$.

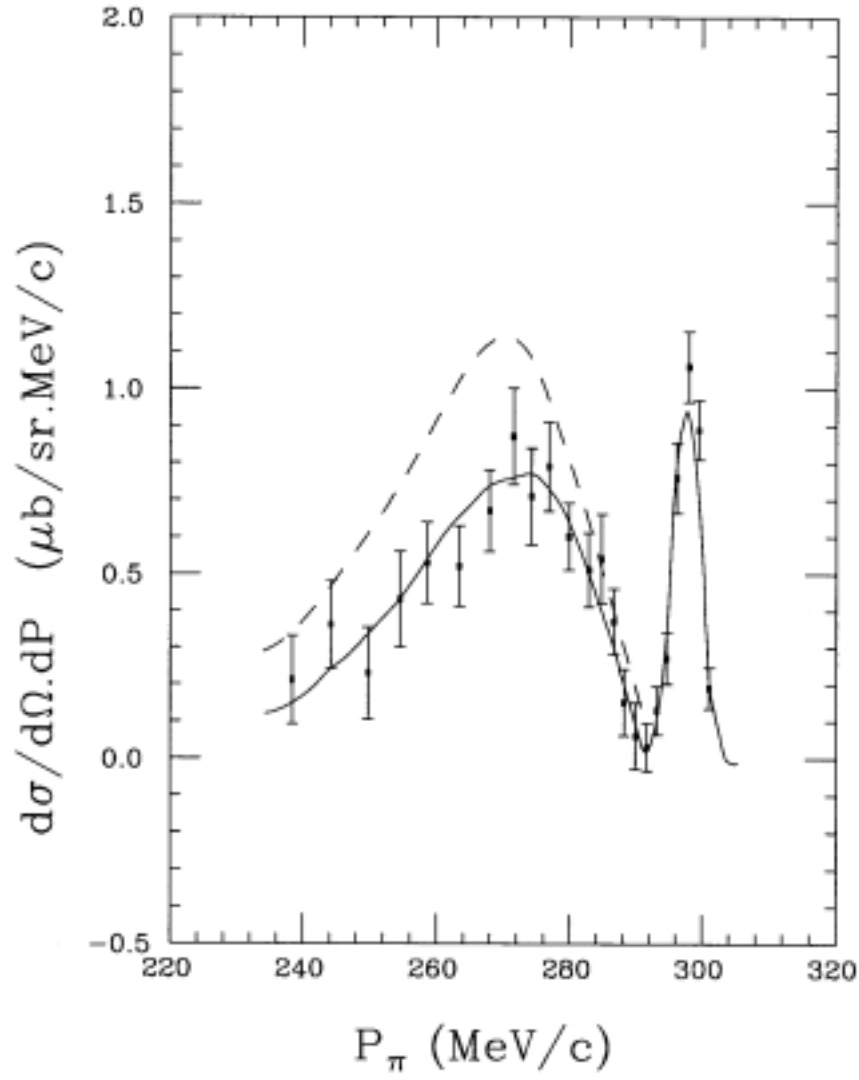


Figure 9: Pion momentum spectrum from Saclay data for $E_\gamma = 338$ MeV and $\theta_\pi = 40.6^\circ$.

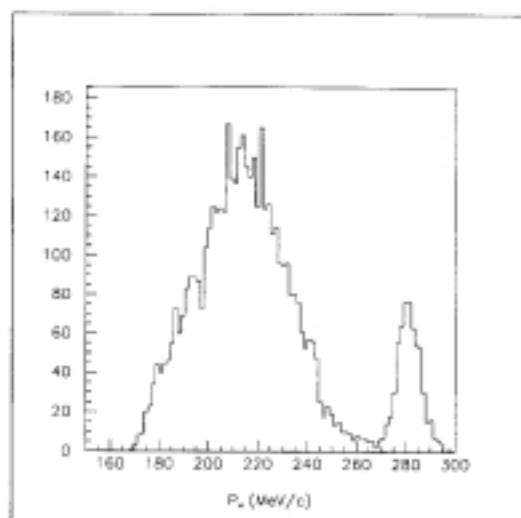


Figure 10: Simulated pion momentum spectrum for $E_\gamma = 350 \text{ MeV}$ and $\theta_\pi = 90^\circ$.

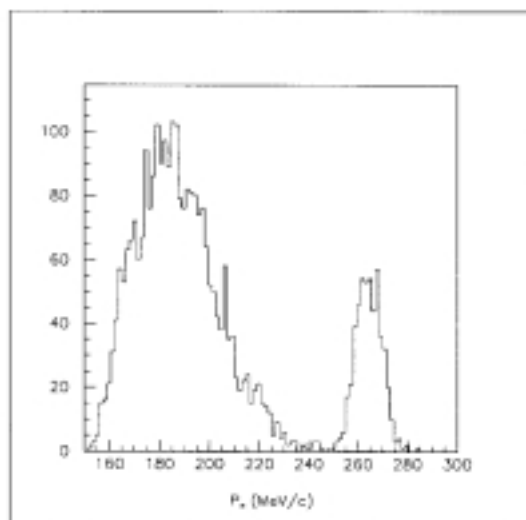


Figure 11: Simulated pion momentum spectrum for $E_\gamma = 350 \text{ MeV}$ and $\theta_\pi = 120^\circ$.

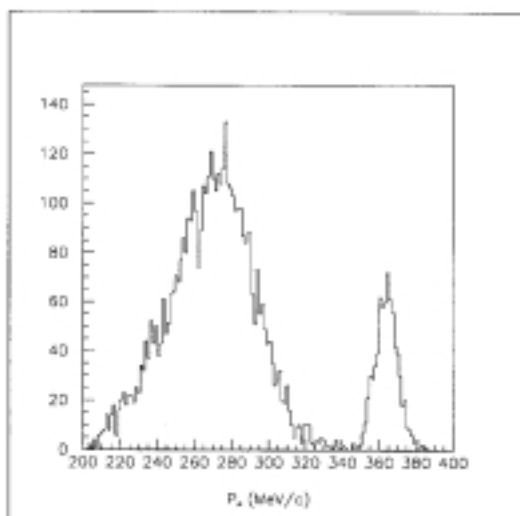


Figure 12: Simulated pion momentum spectrum for $E_\gamma = 450 \text{ MeV}$ and $\theta_\pi = 90^\circ$.

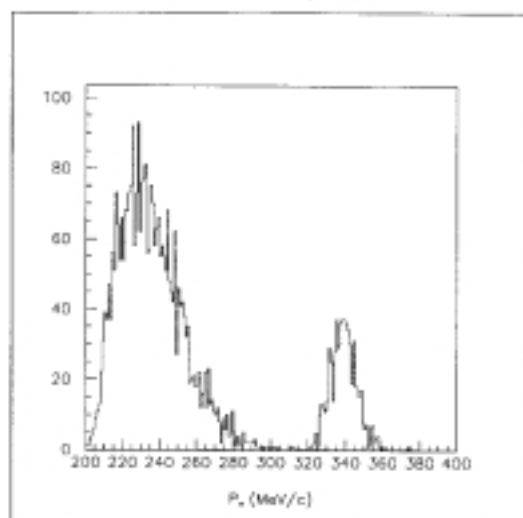


Figure 13: Simulated pion momentum spectrum for $E_\gamma = 450 \text{ MeV}$ and $\theta_\pi = 120^\circ$.

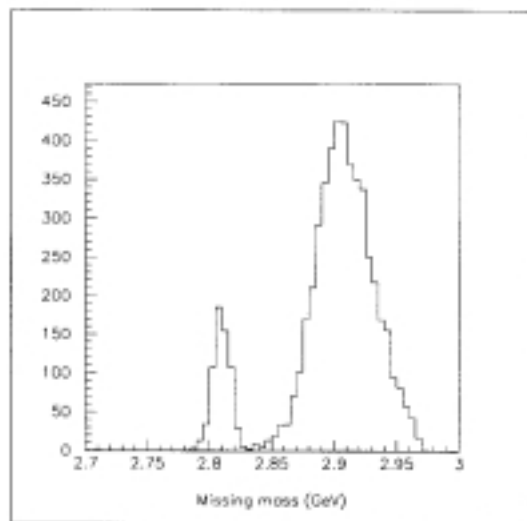


Figure 14: Simulated missing mass spectrum corresponding to an incident photon energy of 450 MeV and a pion emission angle of 90° .

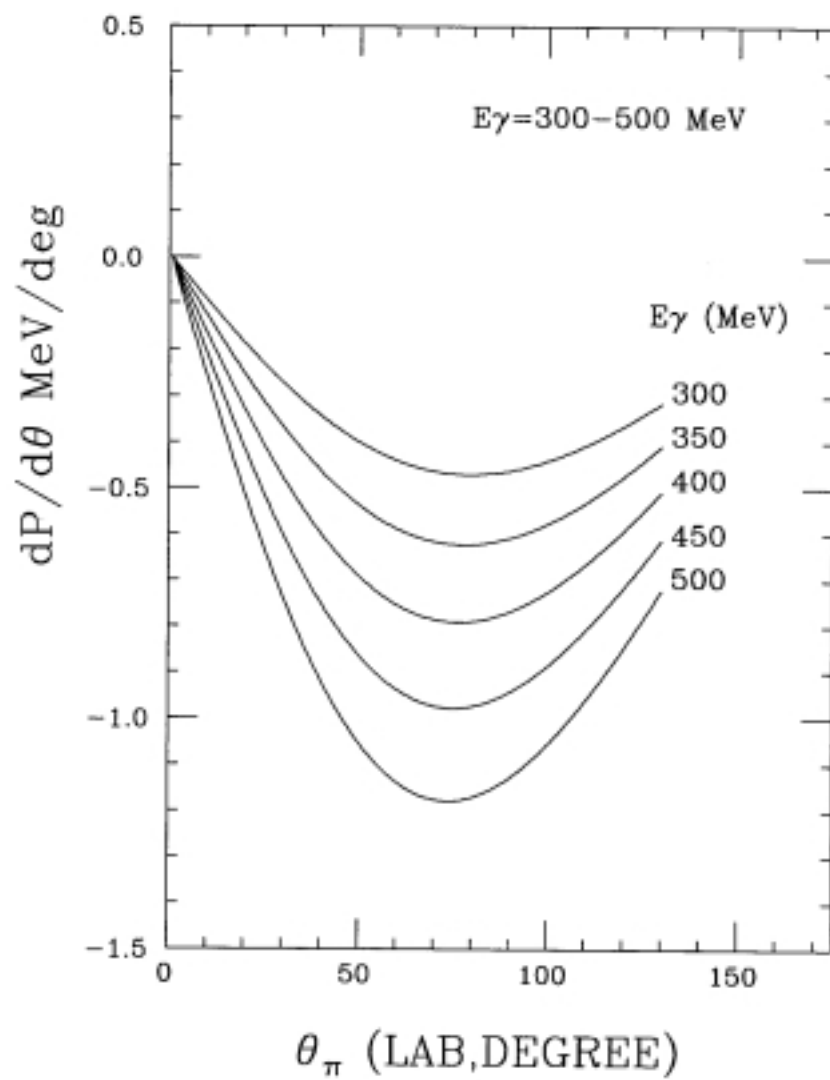


Figure 15: Derivative of pion momentum with respect to emission angle θ_π .

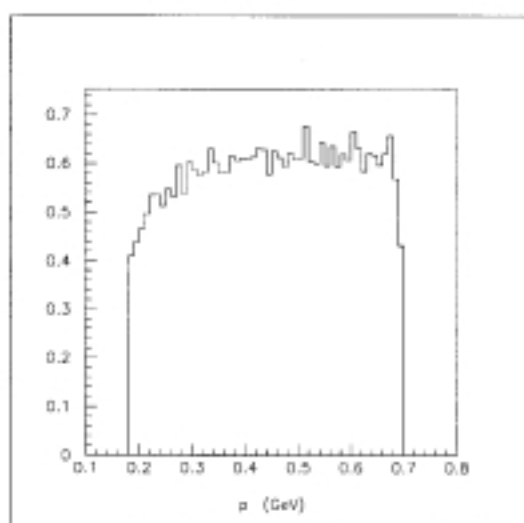


Figure 16: Pion momentum acceptance.

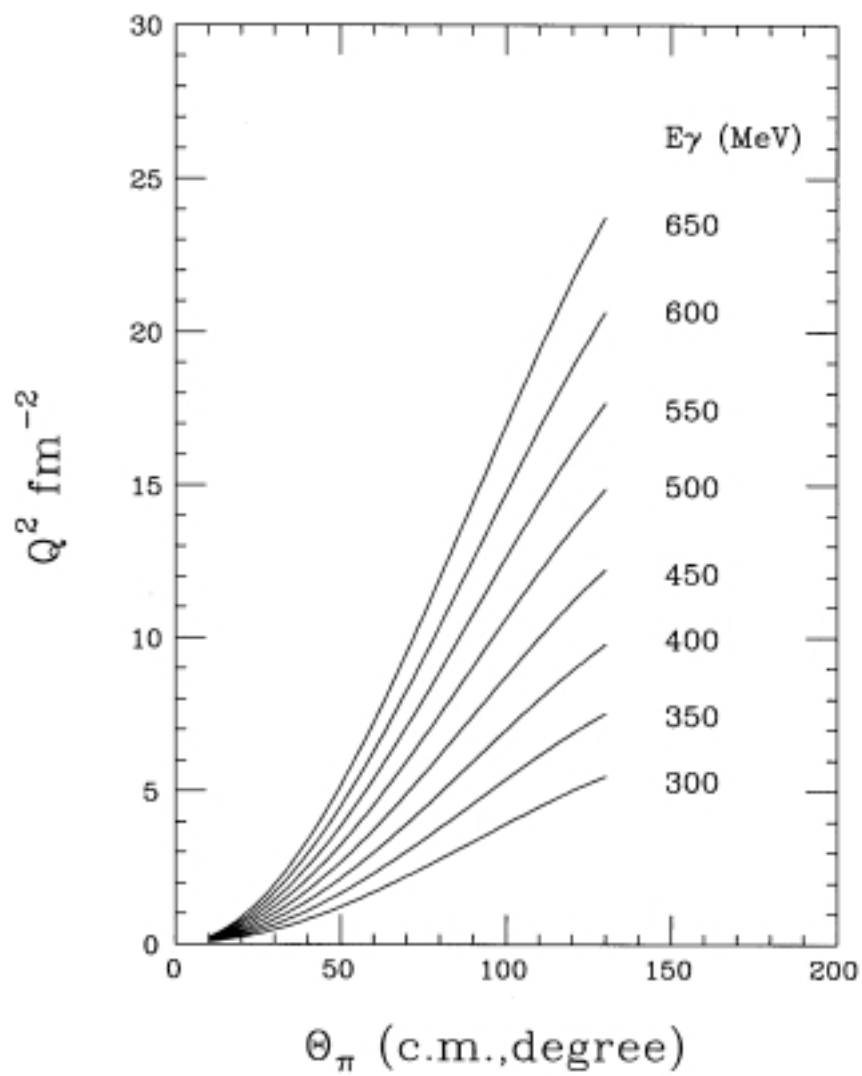


Figure 17: Q^2 dependence on angle Θ_π in c.m. system for different E_γ 's.

3.4 Recoil Detection

As described earlier, the principal particle to be detected is the charged pion. When the π^+ is emitted in the forward direction the kinetic energy of the recoiling ${}^3\text{H}$ is too low to be detected. However, when the π^+ is emitted at backward angles it will be possible to detect the recoiling ${}^3\text{H}$. The main problem in detecting the recoiling ${}^3\text{H}$ is its larger energy loss which will prevent it from reaching the TOF counter.

Table 1 lists the layers of material (composition, distance to target center, thickness, and density) inside the CLAS[22] (including the Čerenkov detector). Table 2 (3) lists the evolution of the energy of a ${}^3\text{H}$ nucleus with an initial kinetic energy of 90 MeV (60 MeV) as it passes through the CLAS with (without) the Čerenkov detector in place. In general, the threshold energy for a ${}^3\text{H}$ to be detected by the CLAS with the Čerenkov detector is about 85 MeV, corresponding to a momentum of 700 MeV/c. The largest energy loss occurs in the Čerenkov detector so if it is removed then the threshold ${}^3\text{H}$ energy can be reduced to about 55 MeV. In addition, if the air gaps could be replaced with helium bags, then the energy losses and, hence, the threshold ${}^3\text{H}$ energy would be further decreased. Figure 18 shows the dependence of the ${}^3\text{H}$ kinetic energy on the π^+ emission angle for different γ energies. In order to detect a significant number of ${}^3\text{H}$'s, the γ energy must be greater than 450 MeV without the Čerenkov counter or the polar angle is larger than 45 degree. If the Čerenkov detector is in the way of the recoiling ${}^3\text{H}$, the photon energy must be higher than 550 MeV in order for the ${}^3\text{H}$ to have enough energy to be detected by the TOF counter.

The principal advantage to be gained by the detection of a recoiling nuclear product will be the suppression of backgrounds, especially when the γ energy is highest and the cross section is the smallest. The detection of a recoiled proton or deuteron will indicate the event is from an inelastic process.

Layer	Item	Material	Distance [cm]	Thickness [cm]	Density [g/cm ³]
1	target	L^3He	0	1.0	0.064
2	cell	mylar	1.0	0.017	1.39
3	pipe	C-fiber	9.5	0.1	1.65
4	gap	air	9.5	0.8	1.29×10^{-3}
5	start.	scint.	10.3	0.3	1.032
6	gap	air	10.6	89.4	1.29×10^{-3}
7	reg. 1	mylar	100	0.0025	1.39
8	reg. 1	Ar-CO ₂	100	15	1.57×10^{-3}
9	reg. 1	mylar	115	0.0025	1.39
10	gap	air	115	40	1.29×10^{-3}
11	reg. 2	nylon	155	0.0016	1.13
12	reg. 2	Ar-CO ₂	155	30	1.57×10^{-3}
13	reg. 2	nylon	185	0.0016	1.13
14	gap	air	185	65	1.29×10^{-3}
15	reg. 3	nylon	250	0.0016	1.13
16	reg. 3	Ar-CO ₂	250	60	1.57×10^{-3}
17	reg. 3	nylon	310	0.0016	1.13
18	gap	air	310	90.0	1.29×10^{-3}
19	Čer	C ₄ F ₁₀	400	70.0	1.29×10^{-3}
20	Čer	CH	470	1.0	1.03
21	gap	air	471	29.0	1.29×10^{-3}
22	TOF	scint.	520	5.0	1.032

Table 1: Material in the path of a particle in the CLAS.

Layer	Material	dE/dx [MeV/cm]	ΔE [MeV]	E_{res} [MeV]	TOF [ns]
1	L^3He	1.6425	1.6425	88.3575	0.0000
2	mylar	23.4211	0.3982	87.9593	0.1363
3	C-fiber	27.4491	2.7449	85.2144	1.3126
4	air	0.0215	0.0172	85.1972	1.3126
5	scint	18.7302	5.6190	79.5782	1.4270
6	air	0.0231	2.0616	77.5166	1.4704
7	mylar	25.9399	0.0648	77.4517	14.4214
8	Ar-CO ₂	0.0281	0.4218	77.0299	14.4214
9	mylar	26.2260	0.0656	76.9644	16.6009
10	air	0.0236	0.9425	76.0219	16.6009
11	nylon	22.2027	0.0355	75.9864	22.4489
12	Ar-CO ₂	0.0286	0.8585	75.1278	22.4489
13	nylon	22.5008	0.0360	75.0918	26.8599
14	air	0.0241	1.5681	73.5238	26.8599
15	nylon	22.9478	0.0367	73.4870	36.5169
16	Ar-CO ₂	0.0295	1.7719	71.7151	36.5169
17	nylon	23.3948	0.0374	71.6777	45.5386
18	air	0.0252	2.2645	69.4132	45.5386
19	C ₄ F ₁₀	0.2135	14.9477	54.4655	60.9935
20	CH	37.0572	37.0572	17.4084	82.0492
21	air	0.0822	2.3839	15.0244	82.3728

Table 2: Energy evolution of a 3H nucleus with an initial energy of 90 MeV in the CLAS with the Čerenkov detector. ΔE is the energy loss in each layer and E_{res} is the energy remaining after leaving the layer. The energy of the 3H nucleus as it leaves the air (Layer 21) and enters the TOF counter, 15.02 MeV, is well above the threshold energy (5 MeV) required to trigger the TOF counter.

Layer	Material	dE/dx [MeV/cm]	ΔE [MeV]	E_{res} [MeV]	TOF [ns]
1	L^3He	2.3220	2.3220	57.6780	0.0000
2	mylar	33.1542	0.5636	57.1144	0.1678
3	C-fiber	39.6371	3.9637	53.1507	1.6449
4	air	0.0319	0.0255	53.1251	1.6449
5	scint	28.6945	8.6083	44.5168	1.7964
6	air	0.0377	3.3724	41.1444	1.8555
7	mylar	43.5829	0.1090	41.0354	19.4800
8	ArCO ₂	0.0467	0.7007	40.3347	19.4800
9	mylar	44.1551	0.1104	40.2243	22.4661
10	air	0.0403	1.6139	38.6105	22.4661
11	nylon	38.8920	0.0622	38.5482	30.5969
12	ArCO ₂	0.0495	1.4846	37.0636	30.5969
13	nylon	40.2331	0.0644	36.9992	36.8188
14	air	0.0438	2.8496	34.1496	36.8188
15	nylon	42.9153	0.0687	34.0810	50.8541
16	ArCO ₂	0.0559	3.3512	30.7298	50.8541
17	nylon	46.9387	0.0751	30.6547	64.5022
18	air	0.0580	11.0283	19.6264	64.5022

Table 3: Energy evolution of a 3H nucleus with an initial energy of 60 MeV in the CLAS with the Čerenkov detector. ΔE is the energy loss in each layer and E_{res} is the energy remaining after leaving the layer. The energy of the 3H nucleus as it leaves the air (Layer 21) and enters the TOF counter, 19.63 MeV, is well above the threshold energy (5 MeV) required to trigger the TOF counter.

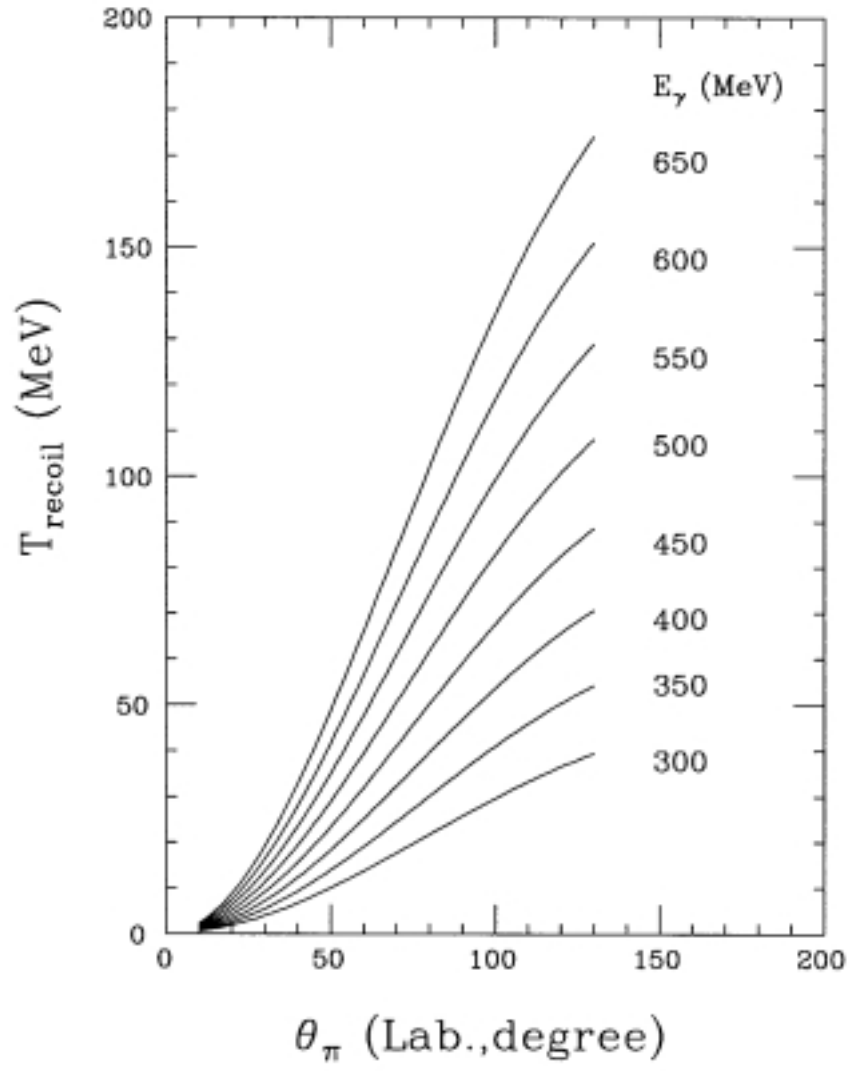


Figure 18: Recoil kinetic energy dependence on θ_{π} for different E_{γ} 's.

3.5 Event Rate and Precision

The time required to obtain a good measurement of the asymmetries can be estimated starting from the cross section and asymmetry at 90° and 120° in the c.m. frame as shown in figures 1 and 2. In these estimates the liquid ^3He target is assumed to be 20 cm long and to have a density of 0.065 g/cm^3 .

The flux distribution and polarization for the Coherent Bremsstrahlung Source was obtained using the code of Jones [23]. The maximum tagged photon flux on target was determined by requiring a trigger rate of not more than 1500 Hz in the CLAS. A collimation angle of one half the characteristic angle was chosen to give good polarization over a reasonable energy range. A total of 300 hours of beam time with a beam energy of 1.6 GeV will be required. The time will be split among the three settings with 20 hours spent at the first setting, 160 hours spent at the second setting, and 120 hours spent at the third setting.

The polarized photon asymmetry Σ is

$$\Sigma = \frac{1}{P_1} \left[\frac{d\sigma/d\Omega^\perp - d\sigma/d\Omega^\parallel}{d\sigma/d\Omega^\perp + d\sigma/d\Omega^\parallel} \right]$$

where the superscripts \perp and \parallel refer to photons polarized perpendicular and parallel to the scattering plane. Since data will be taken for all values of the angle ϕ , the asymmetry is determined by fitting to the complete angular distribution.

The estimated precision of the data for pion emission angles of 90° and 120° is listed in tables 4 and 5. The solid angle was obtained by integrating over 10° bins around the nominal value for θ_π and over the full ϕ_π acceptance. The photon energy was binned in 40 MeV intervals. A 3% systematic uncertainty in the acceptance and normalization was added in quadrature to the statistical uncertainty in computing the error bars for the measurements of the cross section. A 5% systematic uncertainty in the beam polarization was similarly included in the error bars for the photon asymmetry. Projected results are shown in figures 19 through 22 for the differential cross section and the photon asymmetry for pion emission angles of 90° and 120° .

E_γ [MeV]	I_γ [kHz]	P_ℓ [%]	$d\sigma/d\Omega$ [nb/sr]	A_{cp} [%]	Counts [k]	Σ	$\Delta\Sigma$
320.	3720.	0.6000	575.40	76	32.62	0.529	0.0295
360.	2690.	0.8300	113.00	77	4.69	0.593	0.0387
400.	4240.	0.8400	31.06	80	2.11	0.366	0.0410
400.	941.	0.5200	31.06	80	0.47	0.366	0.1271
440.	1853.	0.7300	13.40	82	3.25	-0.171	0.0350
480.	3266.	0.8200	7.47	83	3.23	-0.667	0.0451
520.	1131.	0.6000	5.75	84	0.87	-0.720	0.0876
560.	1997.	0.7400	5.28	84	1.41	-0.449	0.0556
600.	2629.	0.6500	4.57	84	1.60	0.007	0.0543

Table 4: Projected event rates for $\theta_\pi = 90^\circ$. A photon energy range of ± 20 MeV centered on E_γ and a range of scattering angles corresponding to $\pm 5^\circ$ in the c.m. frame was assumed. Incident photon fluxes and polarizations were those determined for the Coherent Bremsstrahlung Source.

The precision of the cross section measurements will be limited mainly by the systematic error to about 4%. The precision of the photon asymmetry measurements will be limited by the systematic 0 at low energies but by statistics at the higher energies. With this precision it will be possible to distinguish the contributions of the E_{1+} multipole and the D-wave. By combining the data taken at all energies and angles we estimate that we will be able to extract the E_{1+} multipole with an uncertainty of 15% and the D-state with an uncertainty of about 5%. These extractions will necessarily be model-dependent but with the large amount of data over such a wide range of kinematics to constrain the fit this dependence should be minimal.

The experiment could also be performed with the proposed Compton High Intensity Photon Source (CHIPS) which would feature high fluxes, low backgrounds, high and much more precisely determined polarization. With a 4.8 GeV electron beam and a 2.4 eV laser, it would be able to deliver at least the 3×10^7 photons per second on target within the energy range of interest required to obtain a total event rate of about 1.5 kHz. The cross section

E_γ [MeV]	I_γ [kHz]	P_ℓ [%]	$d\sigma/d\Omega$ [nb/sr]	A_{cp} [%]	counts [k]	Σ	$\Delta\Sigma$
320.	3720.	0.60	116.80	85	6.81	0.382	0.0344
360.	2690.	0.83	11.51	85	0.49	0.441	0.0803
400.	4240.	0.84	1.44	85	0.10	0.351	0.1723
400.	941.	0.52	1.44	85	0.02	0.351	0.5879
440.	1853.	0.73	0.83	85	0.19	-0.097	0.1409
480.	3266.	0.82	1.14	85	0.46	0.001	0.0804
520.	1131.	0.60	1.36	85	0.19	0.178	0.1707
560.	1997.	0.74	1.48	85	0.37	0.261	0.1004
600.	2629.	0.65	0.79	85	0.26	-0.019	0.1349

Table 5: Projected event rates for $\theta_s = 120^\circ$. A photon energy range of ± 20 MeV centered on E_γ and a range of scattering angles corresponding to $\pm 5^\circ$ in the c.m. frame was assumed. Incident photon fluxes and polarizations were those determined for the Coherent Bremsstrahlung Source.

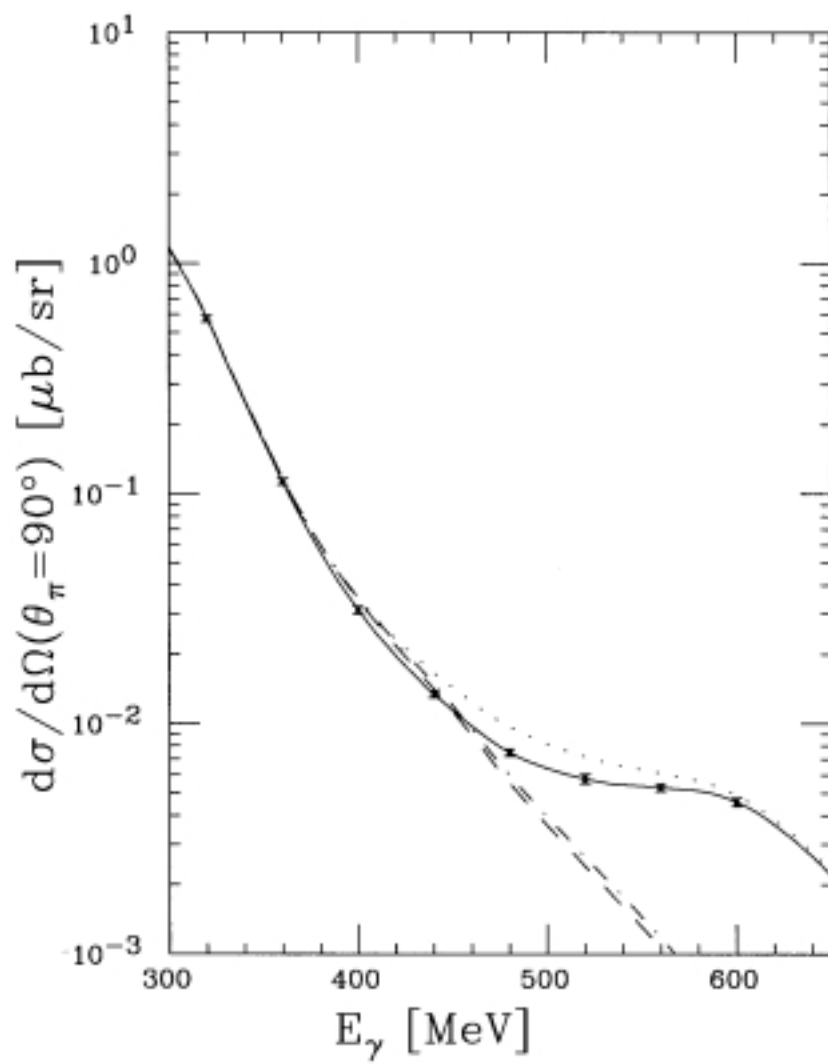


Figure 19: Projected differential cross section measurements at $\theta_\pi = 90^\circ$ for 300 hours of beam from the Coherent Bremsstrahlung Source.

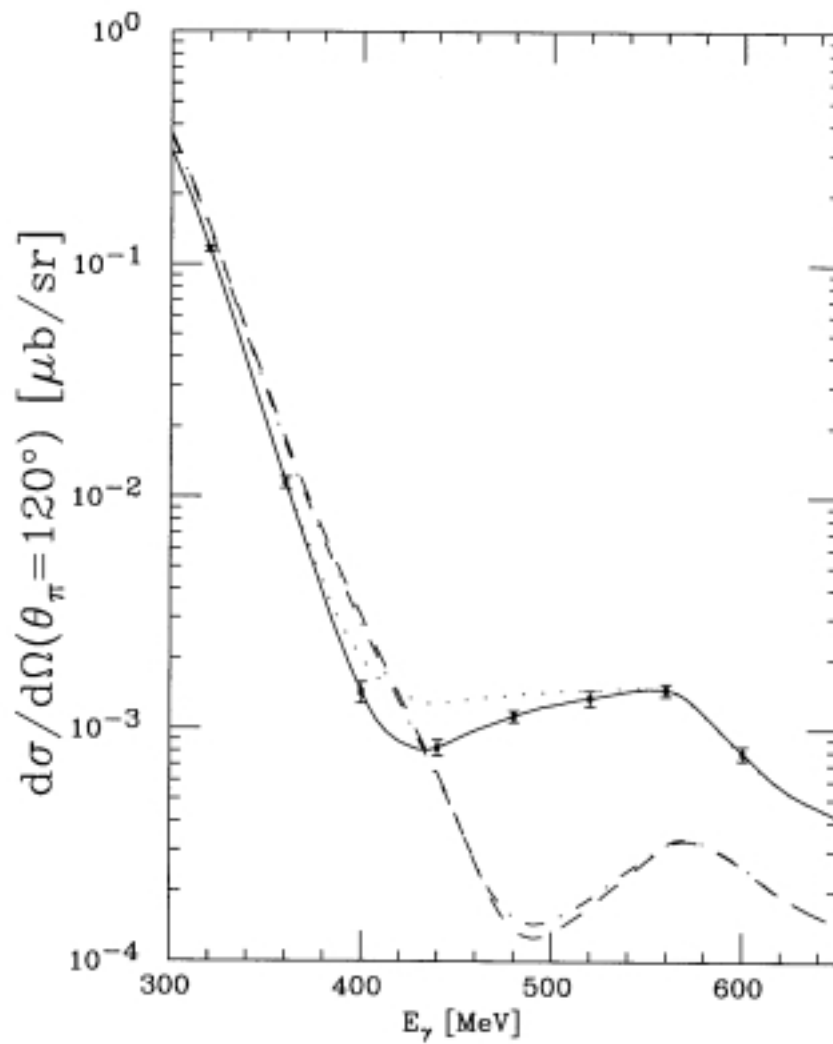


Figure 20: Projected differential cross section measurements at $\theta_\pi = 120^\circ$ for 300 hours of beam from the Coherent Bremsstrahlung Source.

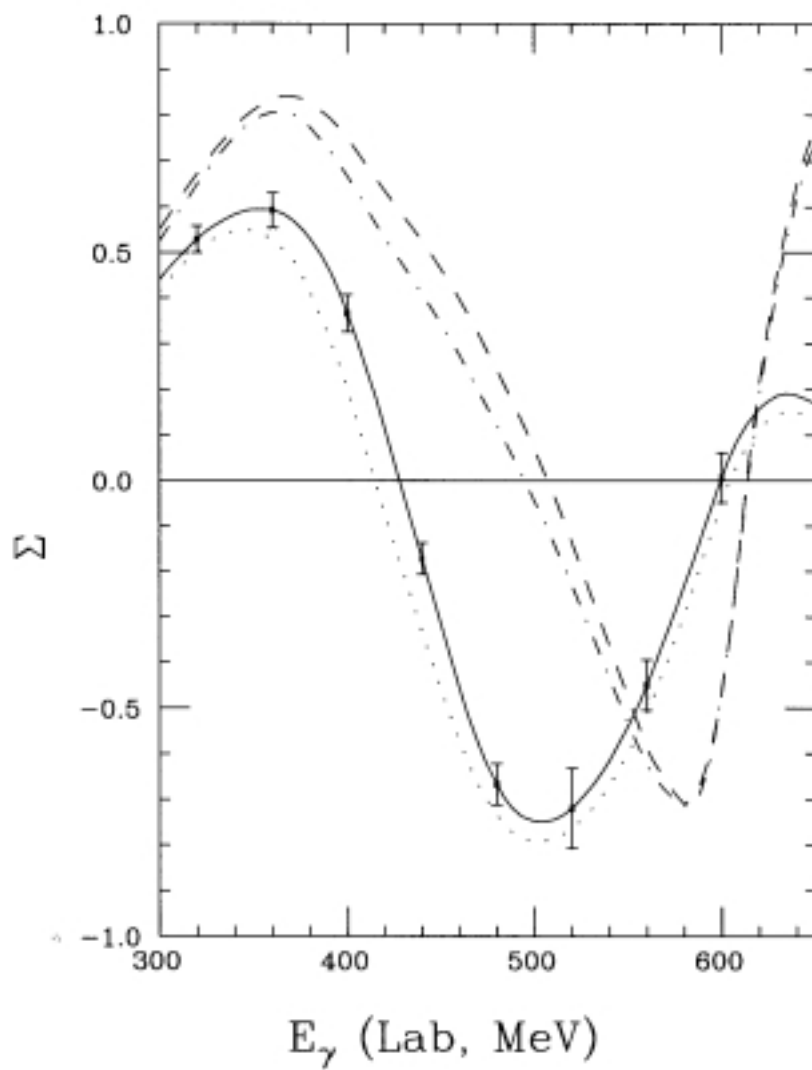


Figure 21: Projected photon asymmetry measurements at $\theta_\pi = 90^\circ$ for 300 hours of beam from the Coherent Bremsstrahlung Source.

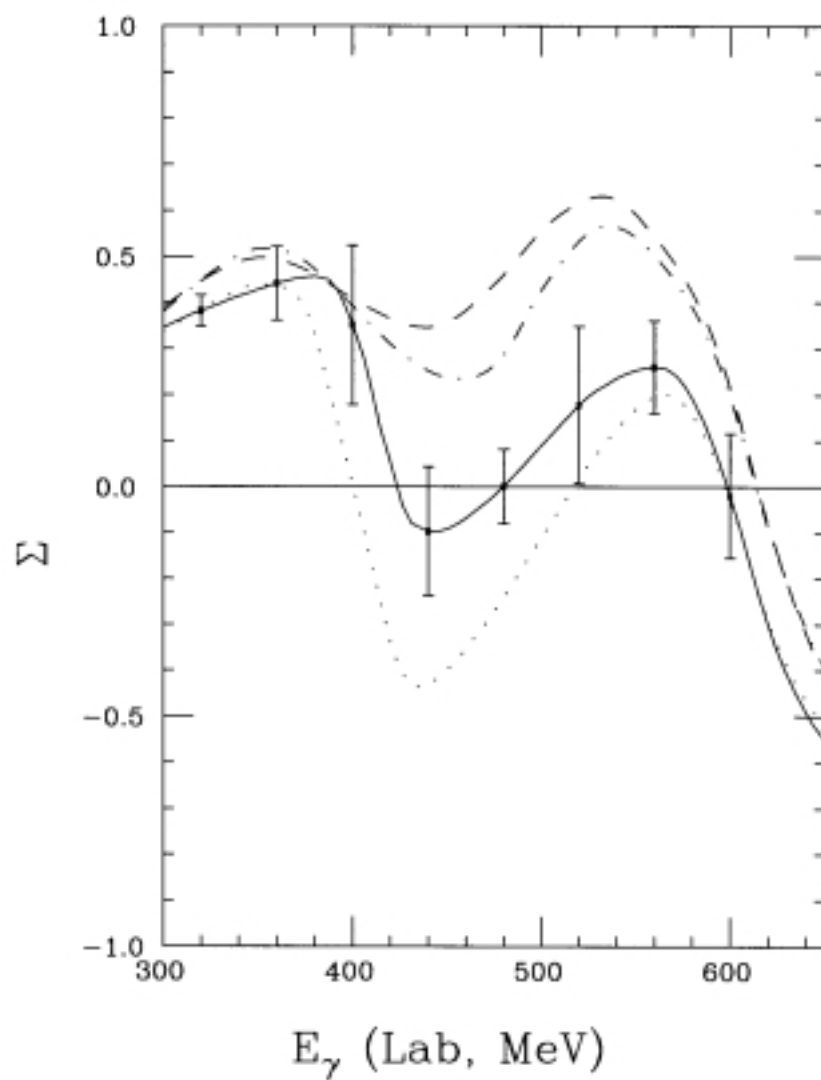


Figure 22: Projected photon asymmetry measurements at $\theta_x = 120^\circ$ for 300 hours of beam from the Coherent Bremsstrahlung Source.

measurements with the CHIPS would also be limited by the 3% systematic uncertainties of the detector system. However, the precision of the photon asymmetry measurements, shown in figures 23 and 24, would be about three times better than the results obtainable with the CBS. This would enable us to extract the $E_{1+}(\Delta)$ with an uncertainty of less than 10% and the D-wave with an uncertainty of less than 5%. Consequently, if the CHIPS is built, it would be the better choice but the physics goals are attainable using either source.

3.6 Additional Accessible Physics

In addition to the reaction upon which this proposal is based, data on several different channels will simultaneously be available:

$$\begin{aligned}
 &^3\text{He}(\vec{\gamma}, \pi^+)nd \\
 &^3\text{He}(\vec{\gamma}, \pi^+n)d \\
 &^3\text{He}(\vec{\gamma}, \pi^+n)pn \\
 &^3\text{He}(\vec{\gamma}, \pi^+d)n \\
 &^3\text{He}(\vec{\gamma}, \pi^+nd) \\
 &^3\text{He}(\vec{\gamma}, \pi^-)ppp \\
 &^3\text{He}(\vec{\gamma}, p)d \\
 &^3\text{He}(\vec{\gamma}, d)p \\
 &^3\text{He}(\vec{\gamma}, p)pn
 \end{aligned}
 \tag{5}$$

First, there are the two- and three-body break-up channels, where meson-exchange currents and possibly off-shell effects may play significant roles [5]. Second, there is the conjugate process, π^- photoproduction. Unlike the π^+ case, no iso-elastic peak in the momentum spectrum can exist. In addition to their intrinsic interest, these data could be useful in fixing the location

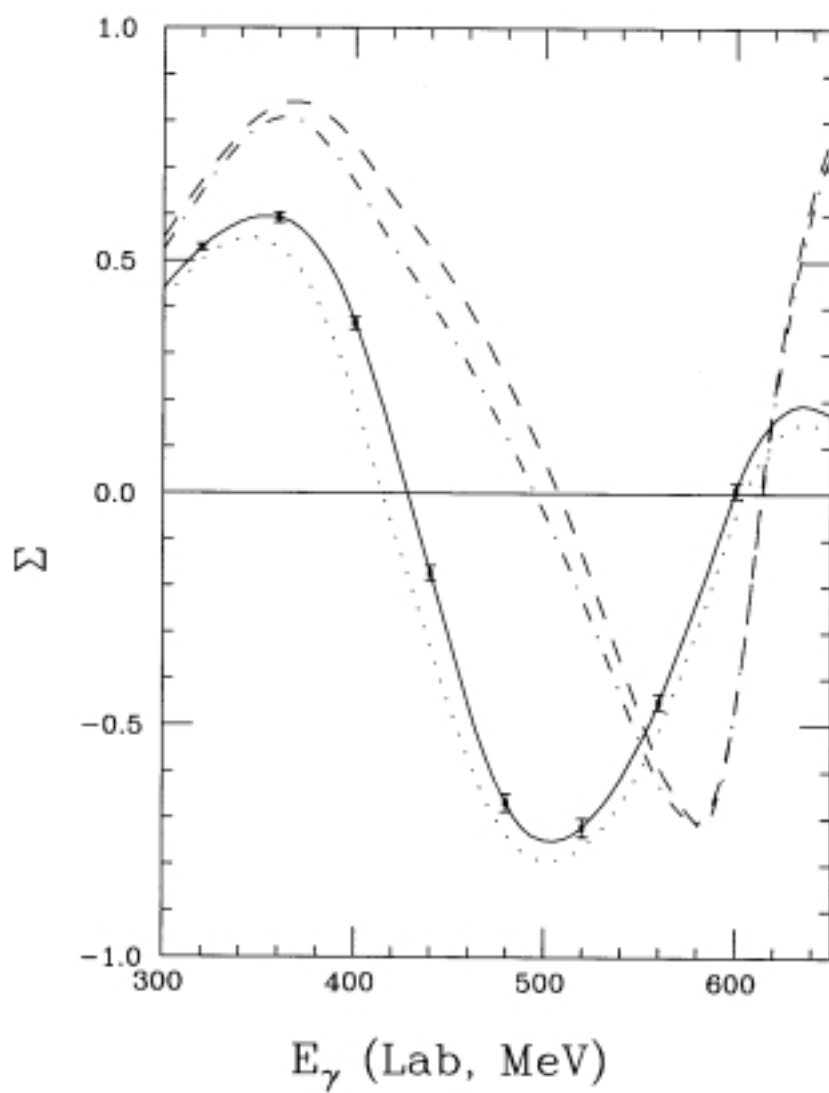


Figure 23: Projected photon asymmetry measurements at $\theta_\pi = 90^\circ$ for 300 hours of beam from the CHIPS.

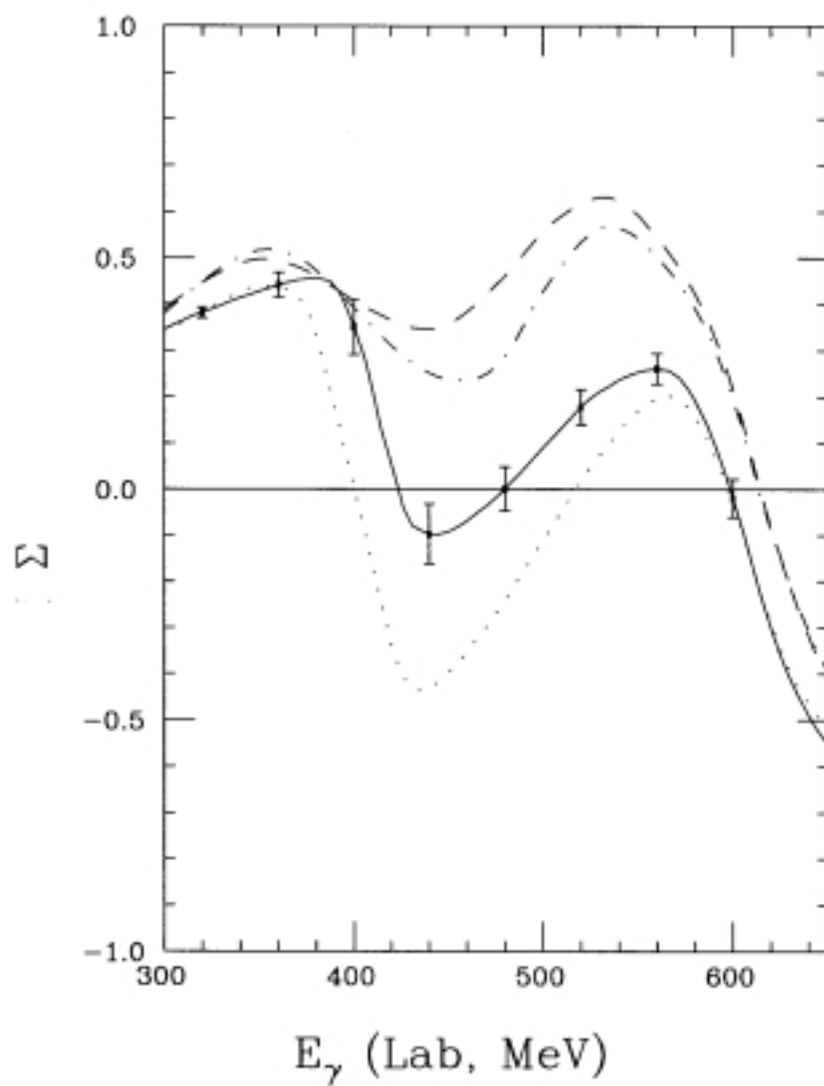


Figure 24: Projected photon asymmetry measurements at $\theta_x = 120^\circ$ for 300 hours of beam from the CHIPS.

of the quasi-free peak and could help us to remove the contributions of the break-up channels from the iso-elastic π^+ production data.

Unfortunately, coherent or elastic π^0 photoproduction will be difficult to measure with any precision. The recoiling ${}^3\text{He}$'s will have energies too low to be detected in the CLAS. The electromagnetic shower counter will be able to detect the two π^0 decay photons but the missing mass resolution is expected to be about 40 MeV, inadequate to isolate elastic events from the two- and three-body photodisintegration channels.

The two-body photodisintegration of ${}^3\text{He}$ has been studied both experimentally and theoretically [24] at lower photon energies. It was found that the meson exchange contribution is very important and that the cross section is very sensitive to the details of the nuclear model. The fit to the data is significantly improved when D-wave components are added to the wave functions. The currently proposed experiment would extend the available data to higher photon energies.

The three-body photodisintegration of ${}^3\text{He}$ has been studied experimentally at Saclay [25]. It was predicted that three-nucleon absorption would play a significant role in the momentum region between the quasi-free and the ${}^3\text{He}(\gamma, p)d$ peaks where the cross section was systematically underestimated by calculation. The experimental data were largely limited by bremsstrahlung contamination in the γ beam. The proposed CHIPS $\vec{\gamma}$ source would not have this problem and the higher quality data may make it possible to clarify this ambiguity.

3.7 Related Experiments

There are two approved experiments in Hall B 0 on photon induced reactions on ${}^3\text{He}$: PR 93-044 and PR 91-014. There is no overlap between the experiment proposed here and these two proposals. First, the two currently approved experiments will use only unpolarized photons; no polarized observables will be measured. Second, they plan to run at significantly higher energies, $E_\gamma > 500\text{MeV}$. Moreover, the physics foci of these experiments,

strange production and three-body break up, are very different from those of the experiment proposed here. A third Hall B experiment, E-89-017, proposes to study the electroexcitation of the Δ in ${}^3\text{He}$ but it also will not involve any polarization measurements and will focus instead on the Q^2 evolution of the production amplitudes.

3.8 Choice of Facility

The proposed experiment requires the unique combination of capabilities offered by the CLAS detector and a $\vec{\gamma}$ source in Hall B. The cross sections are small and measurements over a wide range of pion production angles are required so the broad acceptance of the CLAS is crucial. It is necessary to identify iso-elastic events by reconstructing the missing mass accurately so the relatively high precision of the CLAS detector is also required. Finally, the simplicity of the final state of prime interest (${}^3\text{H} + \pi^+$), of which only the π^+ usually will be detected, requires that background levels be kept very low.

We plan to perform the experiment with the Coherent Bremsstrahlung Source as we have determined that it is adequate for our needs and its construction already has been approved and funded. Should the proposed, but neither approved or funded, CHIPS become available we would use it instead as it would enable us to perform a higher precision measurement with the same amount of beam time.

Few other sources of linearly polarized photons either currently exist or are planned[15]; none are suitable for this measurement.

- LEGS: The maximum photon energy at LEGS is approximately 480 MeV with the new frequency doubled laser, insufficient for this experiment. In addition, the energy resolution of the γ beam is about 5.5 MeV. Unless the iso-elastic channel is identified by detecting the recoiling ${}^3\text{H}$ this resolution, coupled with the low resolution of existing detectors at LEGS, is inadequate. The idea of performing the experiment at LEGS using recoil detection was evaluated but the combination of low

γ flux and thin target required to allow the ^3H 's to escape resulted in prohibitively low counting rates.

- GRAAL: The maximum γ energy at GRAAL will be about 1.1 GeV but the energy resolution will be even worse than at LEGS, about 15 MeV. The flux will be comparable to that at LEGS so attempting the measurement using ^3H detection would suffer from the same prohibitively low rates.
- Spring-8: The planned energy resolution is about 20 MeV with fluxes comparable to those of LEGS and GRAAL.
- TUNL/DFELL: The maximum energy of this facility will be about 200 MeV.
- Mainz: The maximum electron energy at Mainz is about 850 MeV and linearly polarized photons are produced by coherent bremsstrahlung from a diamond. The polarization of γ 's with energies above 500 MeV (where the small cross sections make a high figure of merit imperative) produced by an 850 MeV beam are much too low to be useful for the proposed experiment.
- Bonn: The γ energy resolution is 10 MeV and the flux is comparable to LEGS. Accordingly, the need for recoil detection at all kinematics would necessitate the same thin targets and the same prohibitive event rates as at LEGS.

4 Summary

We are requesting 300 hours of beam time for a measurement of cross sections and asymmetries for the reaction ${}^3\text{He}(\vec{\gamma}, \pi^+){}^3\text{H}$ at photon energies between 300 MeV and 650 MeV. The broad kinematic range to be spanned by the data will enable us to access a rich body of physics related to the interaction of photons and pions with nuclei and, most importantly, possible modifications of the properties of the Δ in a dense nuclear system. It will also enable us to measure the D-state component of the 3-body wave function. The measurements require the unique combination of capabilities promised by the CLAS detector and the Coherent Bremsstrahlung Source; they cannot be performed at any other existing or planned facility.

References

- [1] N. Bianchi *et al.*, Phys. Lett. **B309**, 5 (1993).
- [2] J. O'Fallon *et al.*, Phys. Rev. **141**, 889 (1966).
- [3] D. Bachelier, M. Bernas, and J. Boyard, Nucl. Phys. **A251**, 433 (1970).
- [4] S. Kamalov, L. Tiator, and C. Bennhold, Phys. Rev. Lett. **75**, 1288 (1995).
- [5] N. d'Hose *et al.*, Nucl. Phys. **A554**, 679 (1993).
- [6] B. Bellinghausen *et al.*, Nucl. Phys. **A470**, 429 (1987).
- [7] L. Tiator, A. Rej, and D. Drechsel, Nucl. Phys. **A333**, 343 (1980).
- [8] J. Ballot *et al.*, Nucl. Phys. **A395**, 471 (1983).
- [9] S. Kamalov, L. Tiator, and C. Bennhold, Few-Body Systems **10**, 143 (1991).
- [10] J. M. Laget, Nucl. Phys. **A481**, 765 (1988).
- [11] S. Kamalov, L. Tiator, and C. Bennhold, Nucl. Phys. **A547**, 599 (1992).
- [12] C. Bennhold, private communication, 1995.
- [13] N. d'Hose, thesis, 1995, CEN-Saclay.
- [14] D. Bachelier *et al.*, Phys. Lett. **B44**, 44 (1973).
- [15] B. Norum, in Spin Degrees of Freedom in Electromagnetic Nuclear Physics, 1994, ed. by V. Burkert.
- [16] K. S. Dhuga, private communication.
- [17] B. Norum and P. Welch, 1993, letter of intent, 93-012, CEBAF.
- [18] C. Marchand, private communication, 1995, liquid target.
- [19] J. Gomez *et al.*, Phys. Rev. **C54**, 3160 (1996).

- [20] G. Mutchler, private communication, 1995, start counter.
- [21] B. Niczyporuk, private communication, 1995, SDA code.
- [22] E. Smith, private communication, 1995, CLAS detector.
- [23] R. Jones, private communication, 1998, coherent bremsstrahlung calculations.
- [24] J. Laget, *New Vista in Electro-Nuclear Physics*, Plenum Press, 1985, ed. E.L. Tomusiak.
- [25] N. d'Hose *et al.*, *Phys. Rev. Lett.* **63**, 856 (1989).